Bernstein, E., Caudy, A. A., Hammond, S. M., and Hannon, G. J. (2001). Role for a bidentate ribonuclease in the initiation step of RNA interference. *Nature* 409, 363–366.

Bernstein, E., Kim, S. Y., Carmell, M. A., Murchison, E. P., Alcorn, H., Li, M. Z., Mills, A. A., Elledge, S. J., Anderson, K. V., and Hannon, G. J. (2003). Dicer is essential for mouse development. *Nat. Genet.* 35, 215–217.

Boland, A., Tritschler, F., Heimstadt, S., Izaurralde, E., and Weichenrieder, O. (2010). Crystal structure and ligand binding of the MID domain of a eukaryotic Argonaute protein. *EMBO Rep.* 11, 522–527.

Boss, I. W., Plaisance, K. B., and Renne, R. (2009). Role of virus-encoded microRNAs in herpesvirus biology. *Trends Microbiol.* 17, 544–553.

Britten, R. J., and Davidson, E. H. (1969). Gene regulation for higher cells: a theory. *Science* 165, 349–357.

Brown, B. D., Cantore, A., Annoni, A., Sergi, L. S., Lombardo, A., Della Valle, P. D'Angelo, A., and Naldini, L. (2007). A microRNA-regulated lentiviral vector mediates stable correction of hemophilia B mice. *Blood* 110, 4144–4152.

Brown, B. D., Gentner, B., Cantore, A., Colleoni, S., Amendola, M., Zingale, A. Baccarini, A., Lazzari, G. Galli, C., and Naldini, L. (2007). Endogenous microRNA can be broadly exploited to regulate transgene expression according to tissue, lineage and differentiation state. *Nat. Biotechnol.* 25, 1457–1467.

Cawood, R., Chen, H., Carroll, F., Bazan-Peregrino, M., van Rooijen, N., and Seymour, L. W. (2009). Use of tissue-specific microRNA to control pathology of wild-type adenovirus without attenuation of its ability to kill cancer cells. *PLoS Pathog.* 5, e1000440. doi:10.1371/journal.ppat.1000440.

Chendrimada, T. P., Gregory, R. I., Kumaraswamy, E., Norman, J., Cooch, N., Nishikura, K., and Shiekhattar, R. (2005). TRBP recruits the Dicer complex to Ago2 for microRNA processing and gene silencing. *Nature* 436, 740–744.

Choudhuri, S. (2009). Lesser known relatives of miRNA. *Biochem. Biophys. Res. Commun.* 388, 177–180.

Cobb, B. S., Nesterova, T. B., Thompson, E., Hertweck, A., O'Connor, E., Godwin, J., Wilson, C. B., Brockdorff, N., Fisher, A. G., Smale, S. T., and Merkenschlager, M. (2005). T cell lineage choice and differentiation in the absence of the RNase III enzyme Dicer. *J. Exp. Med.* 201, 1367–1373.

Croce, C. M. (2009). Causes and consequences of microRNA dysregulation in cancer. *Nat. Rev. Genet.* 10, 704–714.

Cullen, B. R. (2009). Viral and cellular messenger RNA targets of viral microRNAs. *Nature* 457, 421–425.

Cullen, B. R. (2010). Five questions about viruses and microRNAs. *PLoS Pathog.* 6, e1000787. doi:10.1371/journal.ppat.1000787.

Daniels, S. M., Melendez-Pena, C. E., Scarborough, R. J., Daher, A., Christensen, H. S., El Far, M., Purcell, D. F., Laine, S., and Gatignol, A. (2009). Characterization of the TRBP domain required for dicer interaction and function in RNA interference. *BMC Mol. Biol.* 10, 38.

Fire, A., Xu, S., Montgomery, M. K., Kostas, S. A., Driver, S. E., and Mello, C. C. (1998). Potent and specific genetic interference by double-stranded RNA in *Caenorhabditis elegans*. *Nature* 391, 806–811.

Gottwein, E., and Cullen, B. R. (2008). Viral and cellular microRNAs as determinants of viral pathogenesis and immunity. *Cell Host Microbe* 3, 375–387.

Haase, A. D., Jaskiewicz, L., Zhang, H., Laine, S., Sack, R., Gatignol, A., and Filipowicz, W. (2005). TRBP, a regulator of cellular PKR and HIV-1 virus expression, interacts with Dicer and functions in RNA silencing. *EMBO Rep.* 6, 961–967.

Haasnoot, J., de Vries, W., Geutjes, E. J., Prins, M., de Haan, P., and Berkhout, B. (2007). The Ebola virus VP35 protein is a suppressor of RNA silencing. *PLoS Pathog.* 3, e86. doi:10.1371/journal.ppat.0030086.

Han, J., Lee, Y., Yeom, K. H., Nam, J. W., Heo, I., Rhee, J. K., Sohn, S. Y., Cho, Y., Zhang, B. T., and Kim, V. N. (2006). Molecular basis for the recognition of primary microRNAs by the Drosha-DGCR8 complex. *Cell* 125, 887–901.

Hashimi, S. T., Fulcher, J. A., Chang, M. H., Gov, L., Wang, S., and Lee, B. (2009). MicroRNA profiling identifies miR-34a and miR-21 and their target genes JAG1 and WNT1 in the coordinate regulation of dendritic cell differentiation. *Blood* 114, 404–414.

Huang, J., Wang, F., Argyris, E., Chen, K., Liang, Z., Tian, H., Huang, W., Squires, K. Verlinghieri, G., and Zhang, H. (2007). Cellular microRNAs contribute to HIV-1 latency in resting primary CD4+ T lymphocytes. *Nat. Med.* 13, 1241–1247.

Jinek, M., and Doudna, J. A. (2009). A three-dimensional view of the molecular machinery of RNA interference. *Nature* 457, 405–412.

Jopling, C. L., Schutz, S., and Sarnow, P. (2008). Position-dependent function for a tandem microRNA miR-122-binding site located in the hepatitis C virus RNA genome. *Cell Host Microbe* 4, 77–85.

Jopling, C. L., Yi, M., Lancaster, A. M., Lemon, S. M., and Sarnow, P. (2005). Modulation of hepatitis C virus RNA abundance by a liver-specific MicroRNA. *Science* 309, 1577–1581.

Kash, J. C., Tumpey, T. M., Proll, S. C., Carter, V., Perwitasari, O., Thomas, M. J., Basler, C. F., Palese, P., Taubenberger, J. K., Garcia-Sastre, A., Swayne, D. E., and Katze, M. G. (2006). Genomic analysis of increased host immune and cell death responses induced by 1918 influenza virus. *Nature* 443, 578–581.

Kelly, E. J., Hadac, E. M., Greiner, S., and Russell, S. J. (2008). Engineering microRNA responsiveness to decrease virus pathogenicity. *Nat. Med.* 14, 1278–1283.

Kelly, E. J., Nace, R., Barber, G. N., and Russell, S. J. (2010). Attenuation of vesicular stomatitis virus encephalitis through microRNA targeting. *J. Virol.* 84, 1550–1562.

Kok, K. H., Ng, M. H. Ching, Y. P., and Jin, D. Y. (2007). Human TRBP and PACT directly interact with each other and associate with dicer to facilitate the production of small interfering RNA. *J. Biol. Chem.* 282, 17649–17657.

Landgraf, P., Rusu, M., Sheridan, R., Sewer, A., Iovino, N., Aravin, A., Pfeffer, S., Rice, A., Kamphorst, A. O., Landthaler, M., Lin, C., Socci, N. D., Hermida, L., Fulci, V., Chiaretti, S., Foa, R., Schliwka, J., Fuchs, U., Novosel, A., Muller, R. U., Schermer, B., Bissels, U., Inman, J., Phan, Q., Chien, M., Weir, D. B., Choksi, R., De Vita, G., Frezzetti, D., Trompeter, H. I., Hornung, V., Teng, G., Hartmann, G., Palkovits, M., Di Lauro, R., Wernet, P., Macino, G., Rogler, C. E., Nagle, J. W., Ju, J., Papavasiliou, F. N., Benzing, T., Lichter, P., Tam, W. Brownstein, M. J. Bosio, A. Borkhardt, A. Russo, J. J. Sander, C. Zavolan, M., and Tuschl, T. (2007). A mammalian microRNA expression atlas based on small RNA library sequencing. *Cell* 129, 1401–1414.

Lanford, R. E., Hildebrandt-Eriksen, E. S., Petri, A., Persson, R., Lindow, M., Munk, M. E., Kauppinen, S., and Orum, H. (2010). Therapeutic silencing of microRNA-122 in primates with chronic hepatitis C virus infection. *Science* 327, 198–201.

Lecellier, C. H., Dunoyer, P., Arar, K., Lehmann-Che, J., Eyquem, S., Himber, C., Saib, A., and Voinnet, O. (2005). A cellular microRNA mediates antiviral defense in human cells. *Science* 308, 557–560.

Lee, Y., Ahn, C., Han, J., Choi, H., Kim, J., Yim, J., Lee, J., Provost, P., Radmark, O., Kim S., and Kim, V. N. (2003). The nuclear RNase III Drosha initiates microRNA processing. *Nature* 425, 415–419.

Lee, Y., Hur, I., Park, S. Y., Kim, Y. K., Suh, M. R., and Kim, V. N. (2006). The role of PACT in the RNA silencing pathway. *EMBO J.* 25, 522–532.

Lewin, B. (2004). *Genes.* Upper Saddle River, NJ: Pearson Education, Inc.

Lewis, B. P., Burge, C. B., and Bartel, D. P. (2005). Conserved seed pairing, often flanked by adenosines, indicates that thousands of human genes are microRNA targets. *Cell* 120, 15–20.

Li, Y., Chan, E. Y., Li, J., Ni, C., Peng, X., Rosenzweig, E., Tumpey, T. M., and Katze, M. G. (2010). MicroRNA expression and virulence in pandemic influenza virus-infected mice. *J. Virol.* 84, 3023–3032.

Liou, L. Y., Herrmann, C. H., and Rice, A. P. (2002). Transient induction of cyclin T1 during human macrophage differentiation regulates human immunodeficiency virus type 1 Tat transactivation function. *J. Virol.* 76, 10579–10587.

Lodish, H. F., Zhou, B. Liu, G., and Chen, C. Z. (2008). Micromanagement of the immune system by microRNAs. *Nat. Rev. Immunol.* 8, 120–130.

Lund, E., Guttinger, S., Calado, A., Dahlberg, J. E., and Kutay, U. (2004). Nuclear export of microRNA precursors. *Science* 303, 95–98.

Macrae, I. J., Zhou, K. Li, F., Repic, A., Brooks, A. N., Cande, W. Z., Adams, P. D., and Doudna, J. A. (2006). Structural basis for double-stranded RNA processing by Dicer. *Science* 311, 195–198.

Matskevich, A. A., and Moelling, K. (2007). Dicer is involved in protection against influenza A virus infection. *J. Gen. Virol.* 88, 2627–2635.

Morris, K. V., and Rossi, J. J. (2006). Lentiviral-mediated delivery of siRNAs for antiviral therapy. *Gene Ther.* 13, 553–558.

Muljo, S. A., Ansel, K. M., Kanellopoulou, C., Livingston, D. M., Rao, A., and Rajewsky, K. (2005). Aberrant T cell differentiation in the absence of Dicer. *J. Exp. Med.* 202, 261–269.

O'Connell, R. M., Rao, D. S., Chaudhuri, A. A., and Baltimore, D. (2010). Physiological and pathological roles for microRNAs in the immune system. *Nat. Rev. Immunol.* 10, 111–122.

Otsuka, M., Jing, Q. Georgel, P., New, L., Chen, J., Mols, J., Kang, Y. J., Jiang, Z., Du, X., Cook, R., Das, S. C. Pattnaik, A. K., Beutler, B., and Han, J. (2007). Hypersusceptibility to vesicular stomatitis virus infection in Dicer1-deficient mice is due to impaired miR24 and

miR93 expression. *Immunity* 27, 123–134.

Pedersen, I. M., Cheng, G., Wieland, S., Volinia, S., Croce, C. M., Chisari, F. V., and David, M. (2007). Interferon modulation of cellular microRNAs as an antiviral mechanism. *Nature* 449, 919–922.

Peng, G., Greenwell-Wild, T., Nares, S., Jin, W., Lei, K. J., Rangel, Z. G., Munson, P. J., and Wahl, S. M. (2007). Myeloid differentiation and susceptibility to HIV-1 are linked to APOBEC3 expression. *Blood* 110, 393–400.

Perez, J. T., Pham, A. M., Lorini, M. H., Chua, M. A., Steel, J., and tenOever, B. R. (2009). MicroRNA-mediated species-specific attenuation of influenza A virus. *Nat. Biotechnol.* 27, 572–576.

Peters, L., and Meister, G. (2007). Argonaute proteins: mediators of RNA silencing. *Mol. Cell* 26, 611–623.

Rossi, J. J., June, C. H., and Kohn, D. B. (2007). Genetic therapies against HIV. *Nat. Biotechnol.* 25, 1444–1454.

Sarasin-Filipowicz, M., Krol, J., Markiewicz, I., Heim, M. H., and Filipowicz, W. (2009). Decreased levels of microRNA miR-122 in individuals with hepatitis C responding poorly to interferon therapy. *Nat. Med.* 15, 31–33.

Selbach, M., Schwanhausser, B., Thierfelder, N., Fang, Z., Khanin, R., and Rajewsky, N. (2008). Widespread changes in protein synthesis induced by microRNAs. *Nature* 455, 58–63.

Sohn, S. Y., Bae, W. J., Kim, J. J., Yeom, K. H., Kim, V. N., and Cho, Y. (2007). Crystal structure of human DGCR8 core. *Nat. Struct. Mol. Biol.* 14, 847–853.

Sung, T. L., and Rice, A. P. (2009). miR-198 inhibits HIV-1 gene expression and replication in monocytes and its mechanism of action appears to involve repression of cyclin T1. *PLoS Pathog.* 5, e1000263. doi:10.1371/journal.ppat.1000263.

Triboulet, R., Mari, B., Lin, Y. L., Chable-Bessia, C., Bennasser, Y., Lebrigand, K., Cardinaud, B., Maurin, T., Barbry, P., Baillat, V., Reynes, J., Corbeau, P., Jeang, K. T., and Benkirane, M. (2007). Suppression of microRNA-silencing pathway by HIV-1 during virus replication. *Science* 315, 1579–1582.

Tsunetsugu-Yokota, Y. (2008). "Transmission of HIV from dendritic cells to CD4+ T cells: a promising target for vaccination and therapeutic intervention," in *AIDS Vaccines, HIV Receptors and AIDS Research*, ed. L. B. Kendow (New York: Nova Science Publishers, Inc.), 117–128.

Wang, X., Ye, L., Hou, W., Zhou, Y., Wang, Y. J., Metzger, D. S., and Ho, W. Z. (2009). Cellular microRNA expression correlates with susceptibility of monocytes/macrophages to HIV-1 infection. *Blood* 113, 671–674.

Wang, Y., Sheng, G., Juranek, S., Tuschl, T., and Patel, D. J. (2008). Structure of the guide-strand-containing argonaute silencing complex. *Nature* 456, 209–213.

Winter, J., Jung, S., Keller, S., Gregory, R. I., and Diederichs, S. (2009). Many roads to maturity: microRNA biogenesis pathways and their regulation. *Nat. Cell Biol.* 11, 228–234.

Wu, H., Neilson, J. R., Kumar, P., Manocha, M., Shankar, P., Sharp, P. A., and Manjunath, N. (2007). miRNA profiling of naive, effector and memory CD8 T cells. *PLoS One* 2, e1020. doi:10.1371/journal.pone.0001020.

Xiao, C., and Rajewsky, K. (2009). MicroRNA control in the immune system: basic principles. *Cell* 136, 26–36.

Yamamoto, T., and Tsunetsugu-Yokota, Y. (2008). Prospects for the therapeutic application of lentivirus-based gene therapy to HIV-1 infection. *Curr. Gene Ther.* 8, 1–8.

Zamore, P. D., and Haley, B. (2005). Ribognome: the big world of small RNAs. *Science* 309, 1519–1524.

Conflict of Interest Statement: The authors declare that the research was conducted in the absence of any commercial or financial relationships that could be construed as a potential conflict of interest.

Received: 22 July 2010; paper pending published: 01 August 2010; accepted: 10 August 2010; published online: 27 August 2010.

Citation: Tsunetsugu-Yokota Y and Yamamoto T (2010) Mammalian microRNAs: post-transcriptional gene regulation in RNA virus infection and therapeutic applications. Front. Microbio. 1:108. doi: 10.3389/fmicb.2010.00108

This article was submitted to Frontiers in Virology, a specialty of Frontiers in Microbiology.

Biochemical and Biophysical Research Communications 403 (2010) 40–45

Contents lists available at ScienceDirect

Biochemical and Biophysical Research Communications

journal homepage: www.elsevier.com/locate/ybbrc

Identification of a novel Vpr-binding compound that inhibits HIV-1 multiplication in macrophages by chemical array

Kyoji Hagiwara [a], Tomoyuki Murakami [a,b], Guangai Xue [a,c], Yasuo Shimizu [a], Eri Takeda [a], Yoshie Hashimoto [a], Kaori Honda [d], Yasumitsu Kondoh [d], Hiroyuki Osada [d], Yasuko Tsunetsugu-Yokota [e], Yoko Aida [a,b,*]

[a] Viral Infectious Diseases Research Unit, RIKEN, 2-1 Hirosawa, Wako, Saitama 351-0198, Japan
[b] Laboratory of Viral Infectious Diseases, Department of Medical Genome Sciences, Graduate School of Frontier Science, The University of Tokyo, Wako, Saitama 351-0198, Japan
[c] Japanese Foundation of AIDS Prevention, Tokyo, Japan
[d] Chemical Biology Core Facility, Advanced Science Institute, RIKEN, 2-1 Hirosawa, Wako, Saitama 351-0198, Japan
[e] Department of Immunology, National Institute of Infectious Diseases, Toyama, Shinjuku-ku, Tokyo 162-8640, Japan

ARTICLE INFO

Article history:
Received 2 October 2010
Available online 29 October 2010

Keywords:
HIV-1 inhibitor
Vpr
Chemical array
Vpr-binding compound
Macrophages
Small-molecule affinity beads

ABSTRACT

Although HIV-1 replication can be controlled by highly active anti-retroviral therapy (HAART) using protease and reverse transcriptase inhibitors, the development of multidrug-resistant viruses compromises the efficacy of HAART. Thus, it is necessary to develop new drugs with novel targets. To identify new anti-HIV-1 compounds, recombinant Vpr was purified from transfected COS-7 cells and used to screen compounds by chemical array to identify those that bound Vpr. From this screen, 108 compounds were selected as positive for Vpr binding. Among these, one structurally similar group of four compounds showed anti-HIV activity in macrophages. In particular, compound SIP-1 had high inhibition activity and reduced the levels of p24 by more than 98% in macrophages after 8 or 12 days of infection. SIP-1 had no cytotoxic effects and did not disrupt cell cycle progression or induce apoptosis of Molt-4 and HeLa cell lines as measured by MTT assay, flow-cytometry analysis, and a caspase-3 assay. In addition, SIP-1 specifically bound to Vpr as assessed by photo-cross-linked small-molecule affinity beads. These results suggest that Vpr is a good target for the development of compounds that could potentially inhibit HIV-1 replication. Collectively, our results strongly suggest that chemical array is a useful method for screening anti-viral compounds.

1. Introduction

HIV-1 infection can be controlled with combinations of anti-retroviral drugs. One approach, termed highly active anti-retroviral therapy uses protease and reverse transcriptase inhibitors, which can decrease viremia below the limit of detection and stop disease progression [1,2]. However, due to problems with these drugs, including the development of viral escape mutants [3], the persistence of viral reservoirs [4–6], poor patient compliance due to complex drug regimens [7], and toxic side effects [8], the need for new drugs with novel targets has become apparent. Many steps in the HIV replication cycle, such as viral adsorption, viral entry, virus-cell fusion, viral assembly and disassembly, proviral integration, viral mRNA transcription, and nuclear import of the viral genome, are potential targets for intervention [9]. In addition to specific steps in the viral life cycle, the HIV-1 accessory gene products Vpr, Vif, Nef, and Vpu have recently been highlighted as potential targets for inhibiting HIV-1 infection. In particular, Vpr is an ideal target due to its unique functions, including nuclear import [10], induction of cell cycle arrest at the G_2 phase [11], apoptosis regulation [11–14] and splicing inhibition [15,16]. The identification of interactions between these accessory gene products and critical host factors that are required for HIV-1 replication may provide novel targets for the development of compounds that are potentially capable of inhibiting HIV-1 replication, thereby decreasing the viral burden in cases of drug-resistant HIV-1 infection.

Macrophages are a major target of HIV-1 and serve as a viral reservoir that releases a small number of viral particles in symptomatic carriers [9,17]. Several studies have shown that Vpr is important for nuclear import of the pre-integration complex (PIC) in macrophages [18–21]. Our studies have shown that Vpr is targeted to the nuclear envelope and then transported into the nucleus by importin α alone, in an importin β-independent manner [19,22]. Recently, we also demonstrated that a compound which suppresses the interaction between Vpr and importin α resulted

* Corresponding author at: Viral Infectious Diseases Research Unit, RIKEN, 2-1 Hirosawa, Wako, Saitama 351-0198, Japan. Fax: +81 48 462 4399.
E-mail address: aida@riken.jp (Y. Aida).

0006-291X/$ - see front matter © 2010 Elsevier Inc. All rights reserved.
doi:10.1016/j.bbrc.2010.10.107

in a decrease in HIV-1 replication in macrophages [23,24]. Thus, the inhibition of function of Vpr may targets for development of compounds that are potentially inhibiting HIV-1 replication.

Chemical array represent one of the most promising and high-throughput approaches for screening ligands of proteins of interest [25], and we recently succeeded in obtaining novel anti-viral compounds using this method [26]. In the present study, we screened for Vpr-binding compounds using a chemical array. This screen resulted in the discovery of novel anti-HIV-1 compounds that block viral replication in macrophages.

2. Materials and methods

2.1. Cell culture

COS-7, 293T, HeLa or Molt-4 cells were cultured in Dulbecco's modified Eagle's medium (DMEM) (SIGMA) or RPMI1640 (Invitrogen) containing penicillin, streptomycin and glutamine (PSG, GIBCO) and 10% fetal bovine serum (FBS, SIGMA) at 37 °C for 2 days in 5% CO_2 as previously described [26].

2.2. Construction of expression plasmids

The pCAGGS mammalian vectors [27] encoding Flag-mRFP-Flag-Vpr or Flag-mRFP were constructed as follows: the cDNAs corresponding to full-length HIV-1 Vpr, which encodes a 96-residue protein, and the Flag-mRFP gene were amplified by PCR using the primers Xho-Flag-mRFP-F, 5′-AAACTCGAGATGGATT ACAAGGACGACGATGACAAGATGGCCTCCTCCGAGGACGTCATC-3′; Not-Vpr-R, TTTGCGGCCGCCTAGGATCTACTGGCTCCATTTC; and Not-mRFP-R, 5′-AAAGCGGCCGCTTAGGCGCCGGTGGAGTG-3′ (restriction enzyme sites are underlined). PCR amplification was performed with KOD Plus Ver.2 (TOYOBO) using mRFP-Flag-Vpr/pCS2+ as a template. After purification of the products using a MinElute PCR Purification Kit (QIAGEN), the DNA was digested with the appropriate restriction enzymes and cloned into pCAGGS. DNA sequencing was performed, and the predicted amino acid sequence of Vpr completely corresponded to the previous reported sequence of pNL432 [28] (GenBank ID: M19921).

2.3. Expression and purification of Flag-fusion proteins

COS-7 cells (1×10^6 cells) were transfected with 10 μg of the pCAGGS mammalian vector encoding Flag-mRFP-Flag-Vpr (Vpr) or Flag-mRFP (mRFP) using FuGene HD transfection reagent (Roche). Two days after transfection, expressed proteins were purified using ANTI-FLAG M2 agarose (SIGMA) as described previously [26].

2.4. SDS–PAGE and immunoblot analysis

Purified proteins were separated by 15% SDS–PAGE under reducing conditions and stained with Coomassie brilliant blue (CBB). Immunoblot analysis was performed using standard methods as described previously [29] with an anti-Flag monoclonal antibody (MAb), followed by incubation with an anti-mouse IgG-alkaline phosphatase antibody (SIGMA).

2.5. Screening for Vpr-binding compounds by chemical array

The chemical arrays were prepared according to our previous reports [25,30]. Solutions of the 8800 compounds (2.5 mg/ml in DMSO) in the NPDepo (RIKEN Natural Products Depository) were arrayed onto five separate photoaffinity-linker-coated glass slides with a chemical arrayer developed at RIKEN. Screening for Vpr-binding compounds was performed by a chemical array screening method as described previously [26,30].

2.6. Macrophage preparation

Human peripheral blood mononuclear cells (PBMCs) were collected from three healthy donors (Nos.1–3) and isolated on a Ficoll gradient (Immuno-Biological Laboratories). Monocytes were selected from PBMC using MACS CD14 MicroBeads (Miltenyi Biotec) and a MACS Separation column (Miltenyi Biotec) with a Quandro MACS Separation Unit (Miltenyi Biotec) as previously described [19]. Monocytes were cultured for 10 days in RPMI 1640 containing 10% FBS, 5% AB serum and 10 ng/ml of human macrophage-colony stimulating factor (PeproTech EC) to promote differentiation into mature macrophages.

2.7. Viral infection of macrophages

HIV-1 was introduced into 293T cells by transfection of macrophage-tropic pNF462 viruses encoding either wild-type Vpr [31] or a deficient form of the protein [32] as described above. After filtration with a 0.45 μM Millipore filter, viral stocks were titrated by an enzyme-linked immunosorbent assay (ELISA) to determine the relative p24 values as described previously [33]. Differentiated primary macrophages (2×10^5 cells/wells) were infected with HIV-1 (a total of 1 ng of p24) at 37 °C for 1 h. After washing three times with RPMI, the cells were cultured in RPMI containing serial 10-fold dilutions of the different compounds ranging in concentrations from 0 to 50 μM or from 0 to 10 μM. Cell supernatants were collected 4, 8 and 12 days after infection, and the p24 values were calculated by ELISA.

2.8. MTT cell viability assay

Molt-4 cells (1×10^5 cells/well) were cultured in 24 well plate at 37 °C for 2 days in the RPMI1640 containing serially diluted compounds ranging from 0 to 10 μM. MTT analysis was performed using a standard method as described previously [26].

2.9. Cell cycle analysis

HeLa cells (1.6×10^6 cells) were harvested at 48 h in the presence of 10 μM of compound and analyzed by flow cytometry for DNA content as described previously [34].

2.10. Analysis of caspase-3 activation

HeLa cells (2×10^6 cells) were harvested 24 h after the addition of 10 μM of compound, and caspase-3 activity was then determined using a caspase-3/CPP32 fluorometric assay kits (Bio Vision) as described previously [34].

2.11. Photo-cross-linked small-molecule affinity beads assay

Compound was cross-linked to Sepharose beads as described previously [35]. Briefly, *N*-hydroxysuccinimide-activated beads were washed three times with 1 mM aq. HCl and coupling solution (0.1 M $NaHCO_3$, 50% dioxane mixture). A solution of photoaffinity linker in coupling solution was then added to the beads, and the beads were incubated at 37 °C for 2 h on a rotator. After washing five times with coupling solution, the beads were blocked with 1 M ethanolamine in 0.1 M Tris–HCl (pH 8.0) buffer at 37 °C for 1 h on a rotator. Beads were then washed three times with milli-Q water and methanol on a spin column and transferred to a glass sample vial. A methanol solution of the compound was added to beads and the mixture was concentrated and dried *in vacuo*. The

beads were irradiated at 365 nm (4 J/cm^2) with a UV cross-linker and washed with methanol to yield compound cross-linked affinity beads.

Recombinant Vpr or mRFP was incubated with compound cross-linked affinity beads at 4 °C for 16 h. After centrifugation, the beads were washed three times with buffer containing 10 mM Tris (pH 7.8), 150 mM NaCl and 0.05% NP-40. The protein that bound to the compound was then separated by 15% SDS–PAGE and detected by immunoblot analysis using an anti-Flag MAb.

3. Results and discussion

To search for compounds that bound to HIV-1 Vpr using a photo-cross-linked chemical array, plasmid was constructed that express chimeric Vpr protein containing an N-terminal Flag tag and mRFP. As a negative control, an expression vector encoding recombinant Flag-mRFP was constructed. To produce chimeric Vpr and mRFP, recombinant plasmids were transfected to COS-7 cells, and the expression of each protein was examined using confocal microscopy. As shown in Fig. 1A, control mRFP was located both in the nucleus and the cytoplasm (Panel 1). In contrast, Vpr mainly localized in the nucleus (Panel 2), indicating that the recombinant Vpr retained its nuclear transport activity. The expressed proteins were purified using Flag-affinity beads and were examined using SDS–PAGE and immunoblot analysis. Purified mRFP and Vpr were clearly detected as single protein bands with apparent molecular masses consistent with their predicted sequences (Fig. 1B left panel). Immunoblot analysis using an anti-Flag MAb also indicated that the Flag-fusion proteins were purified appropriately (Fig. 1B right panel).

The purified proteins were used to screen Vpr-binding compounds by chemical arrays. Flag-mRFP fusion Vpr or Flag-mRFP were incubated with 8800 compounds from a NPDepo that were immobilized on glass slides in duplicate. "Hit ligands" were detected by merged display analysis as described previously [25,26]. As a result of this analysis, a total of 108 compounds were specifically selected as Vpr binding molecules. Among these, 65 compounds were classified into 11 groups by the similarities in their chemical structures (Fig. 1C). First, we investigated whether compounds typical of these 11 groups could block HIV-1 replication in macrophages. Primary macrophages derived from healthy donor No.1 were infected with the macrophage-tropic pNF462 HIV-1 viruses and cultured in RPMI1640 containing serial 10-fold dilutions of different compounds ranging in concentration from 0 to 50 μM. After 4 and 8 days of infection, viral replication was assayed by p24 ELISA. Among the compounds tested, only one

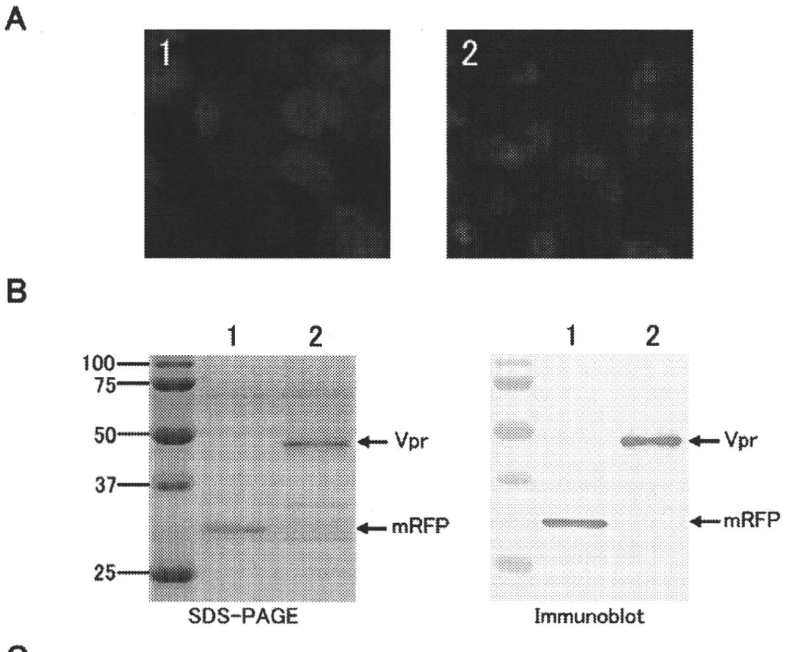

C

	Groups by chemical structures											Others
	1	2	3	4	5	6	7	8	9	10	11	
Number of derivative	6	9	15	11	4	4	3	3	4	3	3	43
Inhibition of HIV-1 replication	–	–	–	–	–	+	–	–	–	–	–	not tested

Fig. 1. Purification of recombinant Vpr protein and chemical array screening. (A) Confocal laser-scanning analysis of recombinant protein localization. COS-7 cells were transfected with pCAGGS mammalian vectors encoding Flag-mRFP (mRFP, Panel 1) or Flag-mRFP-Flag-Vpr (Vpr, Panel 2). (B) SDS–PAGE and immunoblot analysis of purified recombinant proteins. Samples were separated by 15% SDS–PAGE and stained by CBB (left panel). After transferring to a membrane, they were detected by anti-Flag MAb and alkaline phosphatase staining (right panel). Lane 1, purified mRFP; lane 2, purified Vpr. (C) Summary of the screening of compounds by chemical array and inhibitory activities of the compounds. Compounds were classified into 11 groups and the others by the similarities in their chemical structures. Inhibitory activities of the compounds against HIV-1 in macrophages derived from healthy donor No. 1 is shown by + and no activity is shown by –.

belonging to group 6 reduced virus replication efficiently (Fig. 1C) in a dose-dependent manner both on 4 and 8 days after infection (data not shown). This compound showed no cytotoxic effects on Molt-4 cells by MTT assay (data not shown), indicating that the compound has anti-HIV-1 activity.

This compound was designated SIP-1 since it had a basic structure of spiro[1H-indole-3,2′-pyrrolidine]-2-one (Fig. 2A). And we then tested the effect of the other three compounds in the SIP group on HIV-1 replication (Fig. 2B). Primary macrophages derived from healthy donor No. 2 were infected with HIV-1 and cultured in the absence or presence of the compounds at the indicated concentrations for 4, 8 and 12 days. At all time points, macrophages infected with the Vpr^+ virus showed higher p24 values than the macrophages infected with the Vpr^- virus. However, difference of p24 value between two types of viruses was decreased after 12 days infection, suggesting that the Vpr play an important role in early stage of infection in macrophage. As a result, all four compounds inhibited HIV-1 replication on 10 μM treatment at all time points after infection (Fig. 2B). In particular, SIP-1 strongly inhibited viral replication than the other three compounds and reduced the p24 value by approximately 80% at 10 μM. The 50% inhibition concentration (IC_{50}) of SIP-1, SIP-2, SIP-3 and SIP-4 was 5.5, >10, 6.8 and 8.9 μM, respectively, at 8 days post-infection (Table 1). All compounds had no effect of host cell viability as observed by microscopy. In addition, these compounds had no cytotoxic effect on Molt-4 cells as measured by MTT assay (Fig. 2C, Table 1).

To examine the inhibition activity of SIP-1 in more detail, macrophages derived from healthy donor No. 3 were infected with HIV-1. SIP-1 inhibited HIV production by more than 98% at 8 and 12 days post-infection at 10 μM, and at 1 μM reduced viral production by about 80% and 66% at 8 and 12 days post-infection, respectively (Fig. 3A). The IC_{50} of SIP-1 in this assay was 0.5 μM (Table 1) at 8 days post-infection. Different inhibitory effects obtained in Figs. 2 and 3 may be due to distinction of each healthy donor. SIP-1 had no effect on host cell cycle progression as assayed by flow-cytometry analysis (Fig. 3B), or on apoptosis as determined by measurements of caspase-3 activity (Fig. 3C). Collectively, the inhibition of viral replication in infected cells by SIP-1 is due to an ability to inhibit HIV-1 rather than some non-specific cell toxicity since SIP-1 had no advance effect on the cell growth and viability of the cells at 10 μM treatment reaching inhibition levels up to 98%.

Table 1
Summary of the binding and inhibitory activities of the compounds.

Compound[a]	Binding activity to Vpr		IC_{50} (μM)[b]	Cytotoxicity
	Array	Affinity beads		
SIP-1	+[c]	+	5.5 (0.5)	–
SIP-2	+	Not tested	>10	–
SIP-3	+	Not tested	6.8	–
SIP-4	+	Not tested	8.9	–

[a] The Purity of the compounds was greater than 88%.
[b] The IC_{50} compounds after 8 days infection in Fig. 2 is indicated and those of IC_{50} in Fig. 3 is shown in a parenthesis.
[c] Positive activity is shown by + and no activity is shown by –.

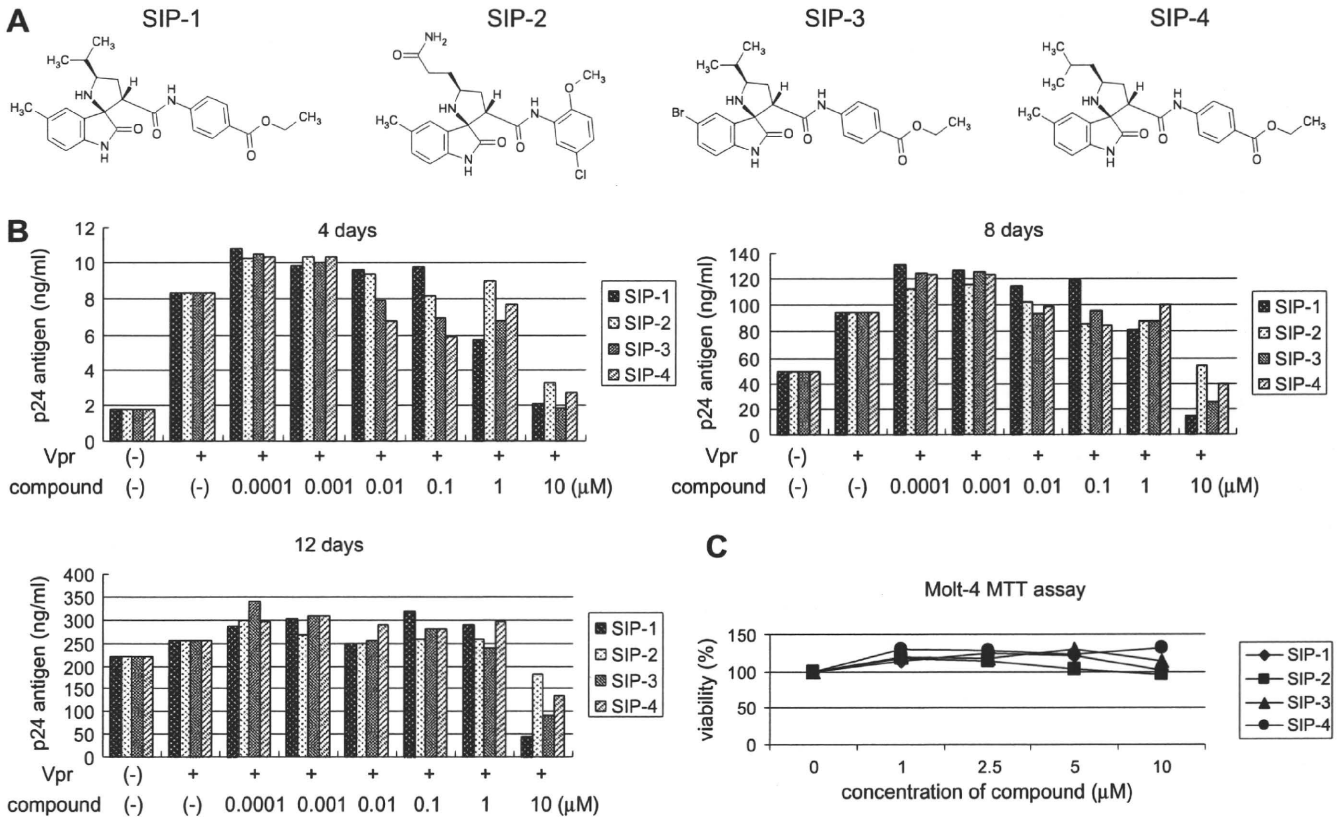

Fig. 2. The effect of different SIP compounds on HIV-1 replication in macrophages and on Molt-4 cell viability. (A) Chemical structures of the compounds screened by chemical arrays. (B) Reduction of viral replication by different SIP compounds. Terminally differentiated primary macrophages derived from healthy donor No.2 were infected by HIV-1 and incubated with serial 10-fold dilutions of compounds ranging in concentration from 0 to 10 μM. The level of virus in the culture supernatants was measured at 4, 8 and 12 days after inoculation by p24 antigen ELISA. The data represent the average p24 value from two wells. (C) The viability of Molt-4 cells was determined by MTT assay following incubation with the SIP compounds. The data represent the average from three wells.

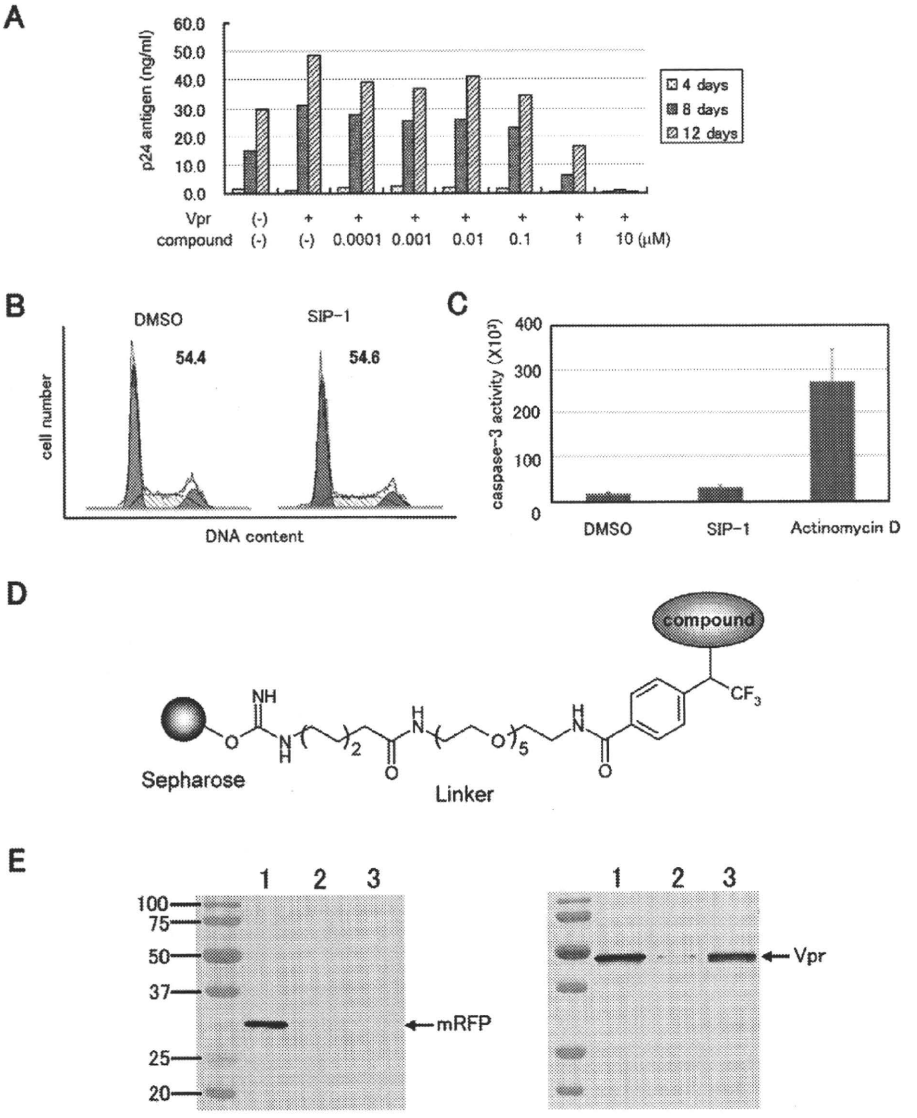

Fig. 3. The effect of SIP-1 on viral replication and normal cell function, and the ability of SIP-1 to bind Vpr. (A) SIP-1-mediated inhibition of viral replication in macrophages. Terminally differentiated primary macrophages derived from healthy donor No. 3 were infected with HIV-1 and then incubated in serial 10-fold dilutions of SIP-1 ranging in concentration from 0 to 10 μM. The levels of virus in the culture supernatants were measured at 4, 8 and 12 days after inoculation by p24 antigen ELISA. The data represent the average p24 value from two wells. (B) Effect of SIP-1 on cell cycle progression. HeLa cells were cultured for 48 h in the presence of 10 μM SIP-1 or DMSO, and cell cycle profiles were analyzed by flow cytometry. The percentage of cells in G1 phase was calculated using ModFit LT Software (Verity Software House) and shown by black bold on the right of each panel. (C) The effect of SIP-1 on apoptosis. HeLa cells were cultured for 24 h in the presence of 10 μM SIP-1, DMSO or Actinomycin D, and caspase-3 activity was determined using a caspase-3/CPP32 fluorometric assay kit (Bio Vision). (D and E) Photo-cross-linked small-molecule affinity beads assay of compound-Vpr binding. A model structure of SIP-1-linked Sepharose beads is shown (D). (E) Purified mRFP (left panel) or Vpr (right panel) was mixed with SIP-1 that had been photo-cross-linked to affinity beads, and then the beads were incubated at 4 °C for 16 h. The proteins that bound to the compound were detected by immunoblot analysis using an anti-Flag MAb followed by incubation with an alkaline phosphatase conjugated antibody. Lane 1, 5% of the total input protein used for the binding assay; lane 2, control beads containing only linker; lane 3, compound-linked beads.

To determine whether SIP-1 directly interacted with Vpr, we performed binding assay using photo-cross-linked small-molecule affinity beads (Fig. 3D and E). Purified Vpr or mRFP was applied to compound-cross-linked affinity beads, and the beads were incubated at 4 °C for 16 h. After sedimentation of the beads, bound proteins were detected by immunoblotting using an anti-Flag MAb. In this assay, recombinant Vpr coprecipitated with compound-linked affinity beads (Fig. 3E lane 3, right panel), whereas control mRFP did not (Fig. 3E left panel), indicating that Vpr specifically binds to the compound.

Together, these results suggest that SIP-1 inhibits Vpr function via binding to its functional domain, thereby inhibiting HIV-1 replication. However, this SIP-1 inhibits which particular function of Vpr is not understood. Therefore, in ongoing studies, we seek to clarify the mechanism of action of SIP group compounds by analyzing the crystal structure of the SIP–Vpr complex. Detailed descriptions of these interactions will provide new therapeutic strategies for rational drug design. Indeed, as the IC_{50} of SIP-1 is approximately 0.5 μM at 8 days after infection, new compound derivatives could potentially develop novel anti-HIV drugs.

4. Conclusions

First, a screen was conducted to identify Vpr-binding compounds using high-throughput chemical arrays. Next, we examined the effect of these compounds on the replication of the macrophage-tropic pNF462 HIV-1 virus in primary macrophages derived from three different human donors. All four SIP group

compounds, which had a basic structure of spiro[1H-indole-3,2′-pyrrolidine]-2-one, inhibited HIV-1 replication in macrophages at 8 or 12 days post-infection and had no cytotoxic effects, indicating that SIP-1-mediated inhibition of viral replication is Vpr-dependent. Finally, assays using photo-cross-linked small-molecule affinity beads indicated that SIP-1 directly binds Vpr, thereby inhibiting HIV-1 replication.

Acknowledgments

We thank Dr. T. Saito for supplying compounds from the NPDepo. This work was supported in part by a Health Sciences Research Grant from the Ministry of Health, Labor and Welfare of Japan (Research on HIV/AIDS) and in part by the Chemical Biology Research Project (RIKEN).

References

[1] G. Barbaro, A. Scozzafava, A. Mastrolorenzo, C.T. Supuran, Highly active antiretroviral therapy: current state of the art, new agents and their pharmacological interactions useful for improving therapeutic outcome, Curr. Pharm. Des. 11 (2005) 1805–1843.
[2] S.G. Deeks, Antiretroviral treatment of HIV infected adults, BMJ 332 (2006) 1489.
[3] G.H. Kijak, J.R. Currier, S. Tovanabutra, J.H. Cox, N.L. Michael, S.A. Wegner, D.L. Birx, F.E. McCutchan, Lost in translation: implications of HIV-1 codon usage for immune escape and drug resistance, AIDS Rev. 6 (2004) 54–60.
[4] J. Kulkosky, S. Bray, HAART-persistent HIV-1 latent reservoirs: their origin, mechanisms of stability and potential strategies for eradication, Curr. HIV Res. 4 (2006) 199–208.
[5] J.D. Siliciano, R.F. Siliciano, Latency and viral persistence in HIV-1 infection, J. Clin. Invest. 106 (2000) 823–825.
[6] N.K. Saksena, S.J. Potter, Reservoirs of HIV-1 in vivo: implications for antiretroviral therapy, AIDS Rev. 5 (2003) 3–18.
[7] D.J. Back, S.H. Khoo, B. Maher, S.E. Gibbons, Current uses and future hopes for clinical pharmacology in the management of HIV infection, HIV Med. 1 (Suppl. 2) (2000) 12-17.
[8] V. Montessori, N. Press, M. Harris, L. Akagi, J.S. Montaner, Adverse effects of antiretroviral therapy for HIV infection, CMAJ 170 (2004) 229–238.
[9] E.O. Freed, A.J. Mouland, The cell biology of HIV-1 and other retroviruses, Retrovirology 3 (2006) 77.
[10] Y. Aida, G. Matsuda, Role of Vpr in HIV-1 nuclear import: therapeutic implications, Curr. HIV Res. 7 (2009) 136–143.
[11] X. Wen, K.M. Duus, T.D. Friedrich, C.M. de Noronha, The HIV1 protein Vpr acts to promote G2 cell cycle arrest by engaging a DDB1 and Cullin4A-containing ubiquitin ligase complex using VprBP/DCAF1 as an adaptor, J. Biol. Chem. 282 (2007) 27046–27057.
[12] A. Azuma, A. Matsuo, T. Suzuki, T. Kurosawa, X. Zhang, Y. Aida, Human immunodeficiency virus type 1 Vpr induces cell cycle arrest at the G(1) phase and apoptosis via disruption of mitochondrial function in rodent cells, Microb. Infect. 8 (2006) 670–679.
[13] M. Nishizawa, M. Kamata, R. Katsumata, Y. Aida, A carboxy-terminally truncated form of the human immunodeficiency virus type 1 Vpr protein induces apoptosis via G(1) cell cycle arrest, J. Virol. 74 (2000) 6058–6067.
[14] B. Schrofelbauer, Y. Hakata, N.R. Landau, HIV-1 Vpr function is mediated by interaction with the damage-specific DNA-binding protein DDB1, Proc. Natl. Acad. Sci. USA 104 (2007) 4130–4135.
[15] C. Hashizume, M. Kuramitsu, X. Zhang, T. Kurosawa, M. Kamata, Y. Aida, Human immunodeficiency virus type 1 Vpr interacts with spliceosomal protein SAP145 to mediate cellular pre-mRNA splicing inhibition, Microb. Infect. 9 (2007) 490–497.
[16] M. Kuramitsu, C. Hashizume, N. Yamamoto, A. Azuma, M. Kamata, Y. Tanaka, Y. Aida, A novel role for Vpr of human immunodeficiency virus type 1 as a regulator of the splicing of cellular pre-mRNA, Microb. Infect. 7 (2005) 1150–1160.
[17] J.M. Orenstein, C. Fox, S.M. Wahl, Macrophages as a source of HIV during opportunistic infections, Science 276 (1997) 1857–1861.
[18] M. Bukrinsky, A. Adzhubei, Viral protein R of HIV-1, Rev. Med. Virol. 9 (1999) 39–49.
[19] Y. Nitahara-Kasahara, M. Kamata, T. Yamamoto, X. Zhang, Y. Miyamoto, K. Muneta, S. Iijima, Y. Yoneda, Y. Tsunetsugu-Yokota, Y. Aida, Novel nuclear import of Vpr promoted by importin alpha is crucial for human immunodeficiency virus type 1 replication in macrophages, J. Virol. 81 (2007) 5284–5293.
[20] S. Popov, M. Rexach, G. Zybarth, N. Reiling, M.A. Lee, L. Ratner, C.M. Lane, M.S. Moore, G. Blobel, M. Bukrinsky, Viral protein R regulates nuclear import of the HIV-1 pre-integration complex, EMBO J. 17 (1998) 909–917.
[21] M.A. Vodicka, D.M. Koepp, P.A. Silver, M. Emerman, HIV-1 Vpr interacts with the nuclear transport pathway to promote macrophage infection, Genes Dev. 12 (1998) 175–185.
[22] M. Kamata, Y. Nitahara-Kasahara, Y. Miyamoto, Y. Yoneda, Y. Aida, Importin-alpha promotes passage through the nuclear pore complex of human immunodeficiency virus type 1 Vpr, J. Virol. 79 (2005) 3557–3564.
[23] T. Suzuki, N. Yamamoto, M. Nonaka, Y. hashimoto, G. Matsuda, S. Takeshima, M. Matsuyama, T. Igarashi, T. Miura, R. Tanaka, S. Kato, Y. Aida, Inhibition of human immunodeficiency virus type-1 (HIV-1) nuclear import via Vpe–Importin interactions as a novel HIV-1 therapy, Biochem. Biophys. Res. Commun. 380 (2009) 838–843.
[24] N. Kanoh, A. Asami, M. Kawatani, K. Honda, S. Kumashiro, H. Takayama, S. Simizu, T. Amemiya, Y. Kondoh, S. Hatakeyama, K. Tsuganezawa, R. Utata, A. Tanaka, S. Yokoyama, H. Tashiro, H. Osada, Photo-cross-linked small-molecule microarrays as chemical genomic tools for dissecting protein–ligand interactions, Chem. Asian J. 1 (2006) 789–797.
[25] G. Xue, Y. Aida, Discovery of a small molecule inhibitor of the interaction between HIV-1 proteins and cellular cofactors: a novel candidate anti-HIV-1 drug, Curr. Chem. Biol. 4 (2010) 188–199.
[26] K. Hagiwara, Y. Kondoh, A. Ueda, K. Yamada, H. Goto, T. Watanabe, T. Nakata, H. Osada, Y. Aida, Discovery of novel antiviral agents directed against the influenza A virus nucleoprotein using photo-cross-linked chemical arrays, Biochem. Biophys. Res. Commun. 394 (2010) 721–727.
[27] H. Niwa, K. Yamamura, J. Miyazaki, Efficient selection for high-expression transfectants with a novel eukaryotic vector, Gene 108 (1991) 193–199.
[28] A. Adachi, H.E. Gendelman, S. Koenig, T. Folks, R. Willey, A. Rabson, M.A. Martin, Production of acquired immunodeficiency syndrome-associated retrovirus in human and nonhuman cells transfected with an infectious molecular clone, J. Virol. 59 (1986) 284–291.
[29] K. Hagiwara, T.U. Ichiki, Y. Ogawa, T. Omura, S. Tsuda, A single amino acid substitution in 126-kDa protein of Pepper mild mottle virus associates with symptom attenuation in pepper; the complete nucleotide sequence of an attenuated strain, C-1421, Arch. Virol. 147 (2002) 833–840.
[30] I. Miyazaki, S. Simizu, H. Ichimiya, M. Kawatani, H. Osada, Robust and systematic drug screening method using chemical arrays and the protein library: identification of novel inhibitors of carbonic anhydrase II, Biosci. Biotechnol. Biochem. 72 (2008) 2739–2749.
[31] M. Kawamura, T. Ishizaki, A. Ishimoto, T. Shioda, T. Kitamura, A. Adachi, Growth ability of human immunodeficiency virus type 1 auxiliary gene mutants in primary blood macrophage cultures, J. Gen. Virol. 75 (1994) 2427–2431.
[32] S. Iijima, Y. Nitahara-Kasahara, K. Kimata, W. Zhong Zhuang, M. Kamata, M. Isogai, M. Miwa, Y. Tsunetsugu-Yokota, Y. Aida, Nuclear localization of Vpr is crucial for the efficient replication of HIV-1 in primary CD4_ T cells, Virology 327 (2004) 249–261.
[33] Y. Tsunetsugu-Yokota, K. Akagawa, H. Kimoto, K. Suzuki, M. Iwasaki, S. Yasuda, G. Hausser, C. Hultgren, A. Meyerhans, T. Takemori, Monocyte-derived cultured dendritic cells are susceptible to human immunodeficiency virus infection and transmit virus to resting T cells in the process of nominal antigen presentation, J. Virol. 69 (1995) 4544–4547.
[34] M. Nonaka, Y. Hashimoto, S. Takeshima, Y. Aida, The human immunodeficiency virus type 1 Vpr protein and its carboxy-terminally truncated form induce apoptosis in tumor cells, Cancer Cell Int. 9 (2009) 20.
[35] N. Kanoh, K. Honda, S. Simizu, M. Muroi, H. Osada, Photo-cross-linked small-molecule affinity matrix for facilitating forward and reverse chemical genetics, Angew. Chem. Int. Ed. 44 (2005) 3559–3562.

Biochemical and Biophysical Research Communications 404 (2011) 822–828

Contents lists available at ScienceDirect

Biochemical and Biophysical Research Communications

journal homepage: www.elsevier.com/locate/ybbrc

Distinct fucosylation of M cells and epithelial cells by Fut1 and Fut2, respectively, in response to intestinal environmental stress

Kazutaka Terahara [a], Tomonori Nochi [b], Masato Yoshida [b], Yuko Takahashi [b], Yoshiyuki Goto [b], Hirotsugu Hatai [b], Shiho Kurokawa [b], Myoung Ho Jang [c], Mi-Na Kweon [d], Steven E. Domino [e], Takachika Hiroi [f], Yoshikazu Yuki [b], Yasuko Tsunetsugu-Yokota [a], Kazuo Kobayashi [a], Hiroshi Kiyono [b,*]

[a] Department of Immunology, National Institute of Infectious Diseases, 1-23-1 Toyama, Shinjuku-ku, Tokyo 162-8640, Japan
[b] Division of Mucosal Immunology, Department of Microbiology and Immunology, The Institute of Medical Science, The University of Tokyo, 4-6-1 Shirokanedai, Minato-ku, Tokyo 108-8639, Japan
[c] Laboratory of Gastrointestinal Immunology, World Premier International Immunology Frontier Research Center, Osaka University, 3-1 Yamada-oka, Suita, Osaka 565-0871, Japan
[d] Mucosal Immunology Section, International Vaccine Institute, Seoul 151-818, Republic of Korea
[e] Department of Obstetrics and Gynecology, The University of Michigan Medical School, 6428 Medical Science Bldg I, 1150 West Medical Center Drive, Ann Arbor, MI 48109-5617, USA
[f] Department of Allergy and Immunology, The Tokyo Metropolitan Institute of Medical Science, 2-1-6 Kamikitazawa, Setagaya-ku, Tokyo 156-8506, Japan

ARTICLE INFO

Article history:
Received 13 December 2010
Available online 21 December 2010

Keywords:
Epithelial cell
Fucosyltransferase
Intestine
M cell
Peyer's patch

ABSTRACT

The intestinal epithelium contains columnar epithelial cells (ECs) and M cells, and fucosylation of the apical surface of ECs and M cells is involved in distinguishing the two populations and in their response to commensal flora and environmental stress. Here, we show that fucosylated ECs (F-ECs) were induced in the mouse small intestine by the pro-inflammatory agents dextran sodium sulfate and indomethacin, in addition to an enteropathogen derived cholera toxin. Although F-ECs showed specificity for the M cell-markers, lectin *Ulex europaeus* agglutinin-1 and our monoclonal antibody NKM 16-2-4, these cells also retained EC-phenotypes including an affinity for the EC-marker lectin wheat germ agglutinin. Interestingly, fucosylation of Peyer's patch M cells and F-ECs was distinctly regulated by α(1,2)fucosyltransferase Fut1 and Fut2, respectively. These results indicate that Fut2-mediated F-ECs share M cell-related fucosylated molecules but maintain distinctive EC characteristics, Fut1 is, therefore, a reliable marker for M cells.

1. Introduction

M cells are generally observed in the follicle-associated epithelium (FAE) of mucosa-associated lymphoid tissues including Peyer's patches (PPs) and isolated lymphoid follicles (ILFs) in the small intestine [1,2], and are morphologically and functionally distinct from their neighboring epithelial cells (ECs) by the presence of relatively short and irregular microvilli on their apical surface and of lymphocytes and antigen-presenting cells frequently enfolded within a pocket structure in their basolateral region [3–5]. In the small intestine of mice, the expression of α(1,2)fucose is believed to be a reliable marker of M cells, because lectin *Ulex europaeus* agglutinin-1 (UEA-1), which has an affinity for α(1,2)fucose, was found to bind exclusively to M cells in the PPs [6,7]. Subsequently, we could found M cells located within the non-FAE-associated small intestinal villous epithelium by utilizing an affinity of UEA-1 [8].

Interestingly, α(1,2)fucosylation is also induced in ileal villous ECs by a variety of intestinal environmental stresses (IES) such as colonization by commensal bacteria, weaning, mechanical injury or treatment with chemicals inhibiting protein synthesis [9–11]. When considering the possible involvement of IES in the development of (or conversion to) M cells, it is reasonable to postulate that such fucosylated ECs form a subset of M cells, because the number of PP M cells is increased rapidly and transiently by alteration from specific pathogen-free (SPF) conditions to a conventional environment [12], by interaction with bacteria such as *Salmonella typhimurium* [13] and *Streptococcus pneumoniae* [14] and during indomethacin-induced ileitis [15]. Like PP M cells, villous M cells might also be induced (or converted) by IES, because a higher frequency of villous M cells is observed in the terminal ileum, which is enriched for commensal bacteria [16]. Recently, we found that some ECs underwent α(1,2)fucosylation in the small intestinal villous epithelium when a mucosal adjuvant cholera toxin (CT) derived from a well known enteropathogen *Vibrio cholerae* was orally administered into mice, and that these cells, in part, shared the same gene expression profile as PP M cells; we previously designated them "M-like cells" [17].

In mice, α(1,2)fucosyltransferase Fut1 and Fut2 are the enzymes responsible for catalyzing an α(1,2) linkage of fucose to terminal β-galactoside, and Fut2 is involved in the IES-associated fucosylation

* Corresponding author. Fax: +81 3 5449 5411.
E-mail address: kiyono@ims.u-tokyo.ac.jp (H. Kiyono).

0006-291X/$ - see front matter © 2010 Elsevier Inc. All rights reserved.
doi:10.1016/j.bbrc.2010.12.067

whereas little is known about Fut1 in the intestine [11,18–20]. In this study, we aimed to elucidate the biological characteristics of ECs that shared the α(1,2)fucose modification with M cells focusing on the fucosylation mechanism, in the hope of better understanding of whether ECs can be reprogrammed into M (or M-like) cells in response to IES.

2. Materials and methods

2.1. Mice

BALB/c and C57BL/6J mice were purchased from SLC (Shizuoka, Japan). Fut1-null and Fut2-null mice (C57BL/6J background) were generated as previously described [21]. These mice were maintained under SPF conditions and used in experiments at 6–9 weeks old. All animal experiments were approved by the Animal Care and Use Committee of The University of Tokyo.

2.2. Lectins and antibodies

The following lectins and antibodies were used for flow cytometry (FCM) and confocal laser scanning microscopy (CLSM): PE-conjugated UEA-1 (UEA-1-PE; Biogenesis, England, UK), tetramethylrhodamine isothiocyanate (TRITC)-conjugated UEA-1 (Vector Laboratories, Burlingame, CA), Alexa Fluor 633-conjugated wheat germ agglutinin (WGA-AF633; Molecular Probes, Eugene, OR), FITC-conjugated NKM 16-2-4 mAb (NKM 16-2-4-FITC) [22], APC-conjugated anti-mouse CD45 mAb (anti-CD45-APC; BD Biosciences, San Jose, CA).

2.3. Alteration of the intestinal environment

A mucosal adjuvant, CT (List Biologic Laboratories, Campbell, CA), and two pro-inflammatory agents, dextran sodium sulfate (DSS, m.w. 36,000–50,000; ICN Biomedicals, Irvine, CA) and indomethacin (Sigma–Aldrich, St. Louis, MO), were used as stress-inducing agents to alter the intestinal environment of mice as described previously [17,23,24] (see Supplementary information).

2.4. Preparation of intestinal epithelial cells for FCM

The small intestinal epithelium was dissociated by a mechanical procedure as described previously [17]. The mononuclear cells were stained with NKM 16-2-4-FITC, UEA-1-PE and anti-CD45-APC and dead cells were stained with 7-aminoactinomycin D (BD Biosciences). Fluorescently labeled cells were analyzed and, if necessary, sort-purified using a FACSAria flow cytometer (BD Biosciences) (see Supplementary information).

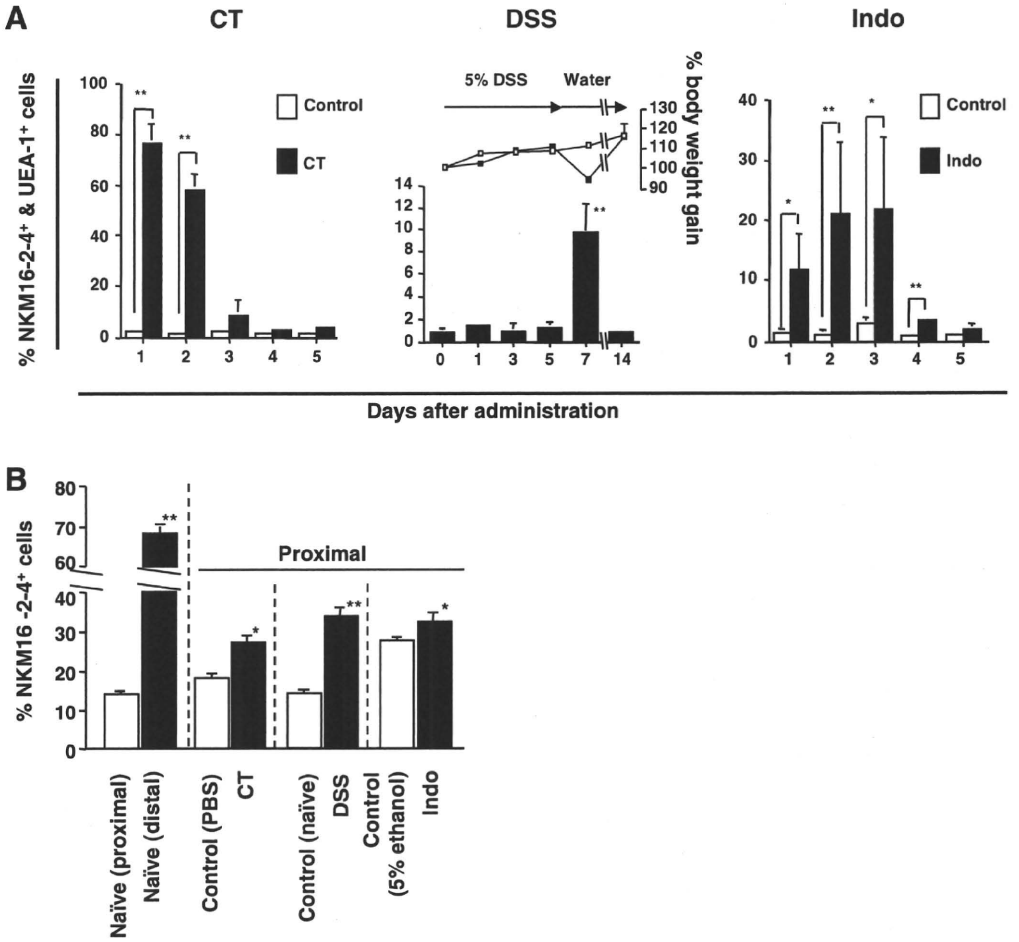

Fig. 1. The influence of IES on the induction of α(1,2)fucosylation in the small intestinal epithelia of BALB/c mice. (A) Daily analysis of the frequency of NKM 16-2-4$^+$/UEA-1$^+$ cells in the proximal villous epithelium of CT-, DSS- and indomethacin (Indo)-administered mice based on FCM. The ratio of NKM 16-2-4$^+$/UEA-1$^+$ cells was enumerated in cells, with 7-aminoactinomycin D$^+$ dead cells, CD45$^+$ leukocytes and small forward- and side-scattered lymphocytes gated out. The line graph in the middle panel shows the percentage body weight gain of control (open squares) and DSS-administered (filled squares) mice. Data are given as means ± SE (n = 3–7). Significant differences (*P < 0.05, **P < 0.01) were determined by t-test or Mann–Whitney's U test. (B) The proportions of NKM 16-2-4$^+$ cells in the PP domes based on histoplanimetrical analysis of CLSM images. Mice used were naïve, or were administered CT (day 1), DSS (day 7) or Indo (day 1). Data are given as means ± SE (n = 3, 19–76 domes). Significant differences (*P < 0.05, **P < 0.01) were determined by t-test.

2.5. Histological analysis

Fluorescently labeled whole-mount tissues were analyzed by CLSM as described previously [8,22]. Each area of NKM 16-2-4$^+$ cells and whole FAE in PPs was quantitated using Scion Image software (Scion Corporation, Frederick, MA) based on the data obtained by CLSM (see Supplementary information).

2.6. Quantitative real-time RT-PCR for Fut1 and Fut2 transcripts

The levels of the *Fut1* and *Fut2* transcripts were quantitated by real-time RT-PCR in the cDNA samples from the sorted cells with reference to the level of hypoxanthine guanine phosphoribosyl transferase (*Hprt*) transcripts (see Supplementary information).

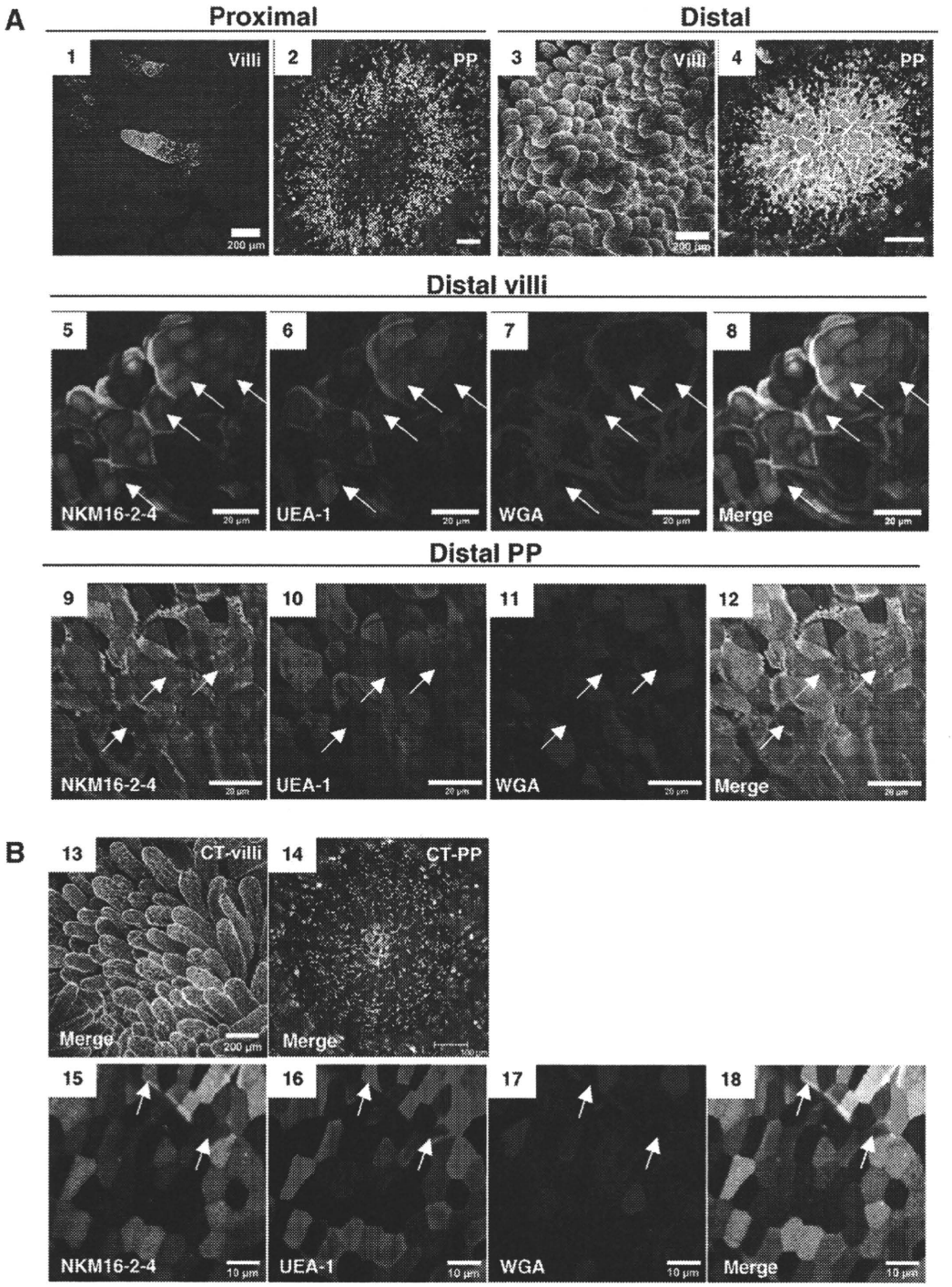

Fig. 2. CLSM analysis of whole-mount small intestinal epithelia of BALB/c mice. Confocal images stained with NKM 16-2-4-FITC, UEA-1-TRITC and WGA-AF633 are shown by green, red and blue, respectively. (A) Proximal villi (1) and PP (2), and distal villi (3, 5–8) and PP (4, 9–12) from naïve mice. (B) Proximal villi (13, 15–18) and PP (14), 1 day after oral CT administration. Arrows show villous M cells (NKM 16-2-4$^+$/UEA-1$^+$/WGA$^-$). Scale bars are 200 μm (1, 3, 13), 100 μm (2, 4, 14), 20 μm (5–12) or 10 μm (15–18). (For interpretation of the references to colour in this figure legend, the reader is referred to the web version of this article.)

2.7. Statistical analysis

The significance of the data was evaluated by the unpaired *t*-test, Mann–Whitney's U test, Tukey's or Scheffé's multiple comparison test based on the normality and variance of the data compared using Statcel2 software (OMS Publishing Inc., Saitama, Japan). $P < 0.05$ was considered statistically significant.

3. Results

3.1. Induction of α(1,2)fucosylation in the small intestinal epithelium by IES

To examine the influence of IES on M cell-associated α(1,2)fucosylation (NKM 16-2-4$^+$/UEA-1$^+$), we focused on the proximal epithelium, where NKM 16-2-4$^+$/UEA-1$^+$ cells were rarely found in naïve mice (Supplementary Fig. S1). When CT was orally administered to BALB/c mice, NKM 16-2-4$^+$/UEA-1$^+$ cells were dramatically increased in the proximal villous epithelium, with an average of 75.9% double-positive cells one day post-inoculation (Fig. 1A). The proportion of NKM 16-2-4$^+$/UEA-1$^+$ cells returned to the control level (approximately 2%) at 3 days post-inoculation. Similarly, a significant increase in NKM 16-2-4$^+$/UEA-1$^+$ cells was observed when pro-inflammatory agents, such as DSS or indomethacin, were administered (Fig. 1A).

A similar tendency was also seen in the FAE of PPs. We next performed histoplanimetrical analysis based on single NKM 16-2-4 signals obtained by CLSM. We previously demonstrated that NKM 16-2-4$^+$ cells included UEA-1$^+$ M cells but not goblet cells [22]. However, similar to UEA-1, because NKM 16-2-4 reacts to Paneth cells (Supplementary Fig. S2), NKM 16-2-4$^+$ cells were enumerated upward the crypts where Paneth cells locally exist. Therefore, goblet cells and Paneth cells were excluded in this analysis. When the proportions of NKM 16-2-4$^+$ cells were compared between the proximal and distal PP FAE of naïve BALB/c mice, a higher frequency of NKM 16-2-4$^+$ cells was observed in the distal (68.4%) than in the proximal (13.9%) PP FAE (Fig. 1B). Furthermore, a significant increase in NKM 16-2-4$^+$ cells was observed in the proximal PP FAE following CT-, DSS- or indomethacin-administration, averaging 27.2% (control: 18.1%), 33.8% (control: 13.9%) and 32.4% (control: 27.5%) positive cells, respectively (Fig. 1B). These results indicate that IES enhances α(1,2)fucosylation in both the PP FAE and the villous epithelium.

3.2. CLSM analysis of IES-induced NKM 16-2-4$^+$/UEA-1$^+$ cells

To assess qualitative cellular traits of IES-induced NKM 16-2-4$^+$/UEA-1$^+$ cells, we performed CLSM analysis using lectin WGA, which has an affinity for ECs and goblet cells but not M cells [6,8]. As indicated by FCM (Supplementary Fig. S1), a higher frequency of NKM 16-2-4$^+$/UEA-1$^+$ cells was observed in the distal (Fig. 2A; 3 and 4) than in the proximal villi and PPs (Fig. 2A; 1 and 2) in naïve BALB/c mice. In general, these NKM 16-2-4$^+$/UEA-1$^+$ cells were preferentially located at the tips of the villi (Fig. 2A; 1 and 3) and PP domes (Fig. 2A; 4) and a large proportion of them showed an affinity for WGA in both the villous epithelium (Fig. 2A; 7) and the PP FAE (Fig. 2A; 11), although a substantial number of villous M cells sharing the typical M cell hallmark (NKM 16-2-4$^+$/UEA-1$^+$/WGA$^-$) existed in the distal villi of naïve mice (Fig. 2A; 5–8: arrows).

The CLSM analysis further demonstrated that CT-induced NKM 16-2-4$^+$/UEA-1$^+$ cells also reacted with WGA (Fig. 2B). In contrast, villous M cells showing the M cell-phenotype (NKM 16-2-4$^+$/UEA-1$^+$/WGA$^-$) remained at a very low frequency irrespective of IES by CT (Fig. 2B; 15–18: arrows). A similar observation was made when DSS or indomethacin was administered (Supplementary Fig. S3). In the proximal PP FAE, whereas a substantial number of NKM 16-2-4$^+$/UEA-1$^+$ cells were negative for WGA and were radially distributed on the dome, indicating an M cell-phenotype (Fig. 2A; 2), triple-positive cells (NKM 16-2-4$^+$/UEA-1$^+$/WGA$^+$) were evident and were located on the tip of the dome after oral CT administration (Fig. 2B; 14). These results indicate that IES-induced NKM 16-2-4$^+$/UEA-1$^+$ cells share an affinity for WGA, a common trait of normal ECs [6], and hardly contain any villous M cells. We thus designated them fucosylated ECs (F-ECs), to distinguish them from typical M cells.

3.3. Different expression patterns of Fut1 and Fut2 transcripts in the small intestinal epithelium

To examine in more detail the mechanism of α(1,2)fucosylation between F-ECs and M cells, we performed quantitative real-time RT-PCR for *Fut1* and *Fut2* transcripts. Quantitative real-time RT-PCR demonstrated that high expression of *Fut1* transcripts was seen only in NKM 16-2-4$^+$/UEA-1$^+$ cells isolated from the naïve PP FAE where M cells predominantly exist (Fig. 3A). On the other hand, elevated expression of *Fut2* transcripts, but not *Fut1* transcripts, was detected in F-ECs located in the distal epithelia of naïve mice (Fig. 3A and B). Similarly, enhanced expression of *Fut2* transcripts, but not *Fut1* transcripts, was seen in CT-, DSS- and indomethacin-induced F-ECs of the proximal epithelia (Fig. 3A and B). These results indicate that α(1,2)fucosylation of F-ECs in the villous epithelium is induced by Fut2, and suggest that Fut1 is expressed in PP M cells irrespective of IES.

3.4. Distinct requirements for Fut1 or Fut2 for α(1,2)fucosylation of M cells or F-ECs, respectively

To clarify the distinct requirements for the Fut isoforms in F-ECs and M cells, Fut1-null and Fut2-null mice were employed for FCM

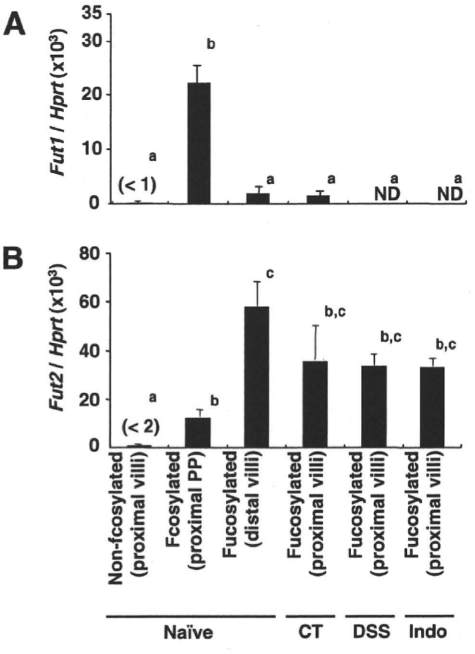

Fig. 3. Quantification of the expression levels of *Fut1* and *Fut2* transcripts relative to levels of *Hprt* transcripts. Fucosylated (NKM 16-2-4$^+$/UEA-1$^+$) and non-fucosylated (UEA-1$^-$) cells were purified from the proximal or distal small intestinal epithelia using a cell-sorter. Naïve, or CT- (Day 2), DSS- (Day 7) or indomethacin (Indo)- (Day 2) treated BALB/c mice were used. (A) *Fut1* transcripts. (B) *Fut2* transcripts. Data are given as means ± SE ($n = 3$–4). Different letters indicate significant differences ($P < 0.05$) determined by Tukey's multiple comparison test.

and CLSM analyses. Because these mice are on a C57BL/6J background [21], wild-type (WT) C57BL/6J mice were employed as a control group. Like BALB/c mice, WT C57BL/6J mice showed a higher frequency of F-ECs (NKM 16-2-4$^+$/UEA-1$^+$ cells) in the distal villous epithelium than in the proximal villous epithelium, and that the frequency of F-ECs in the latter increased after oral CT administration (Fig. 4A). This was also observed when Fut1-null mice were orally exposed to CT (Fig. 4A and C; 2 and 4). On the

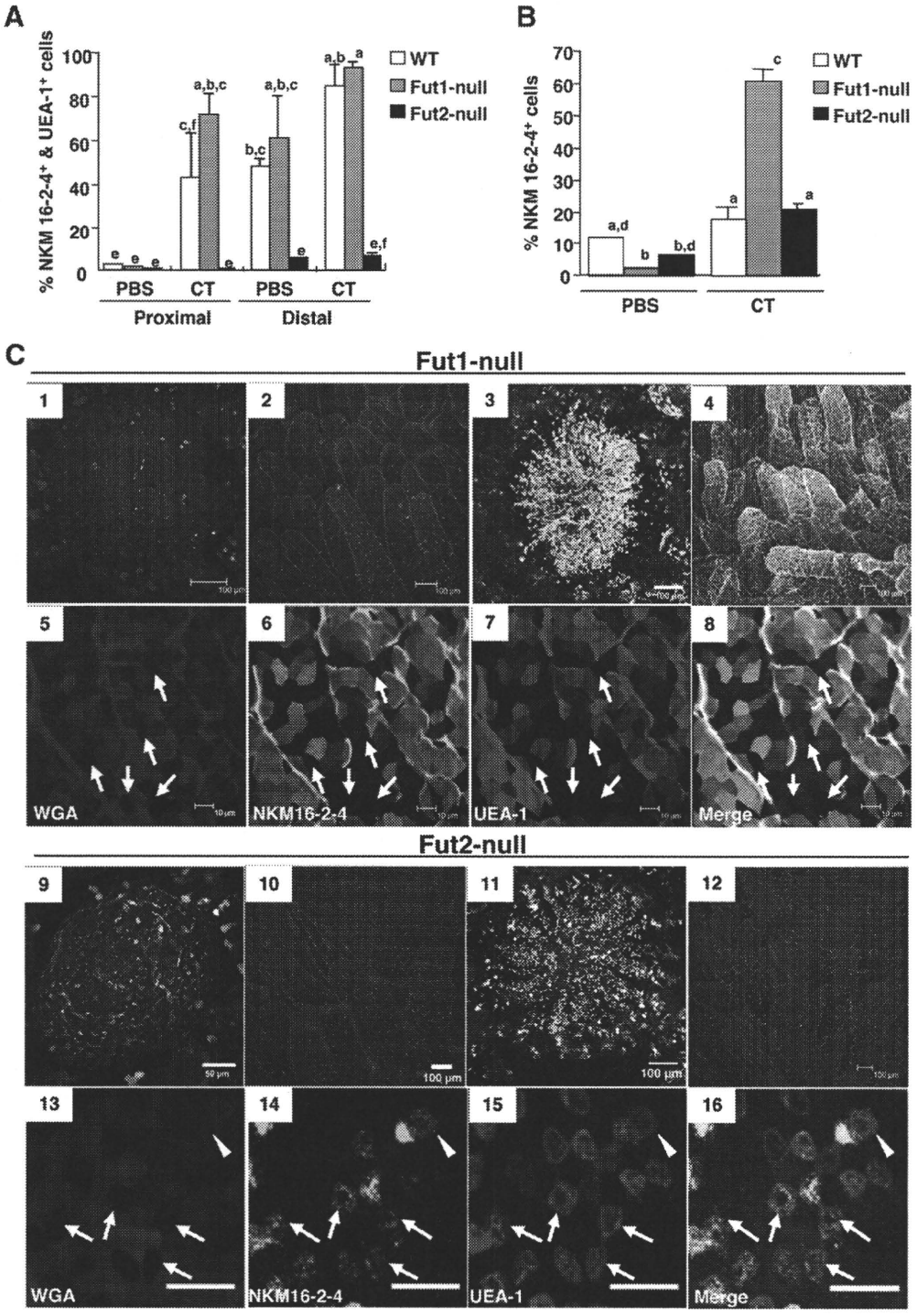

Fig. 4. Fut1- and Fut2-dependent α(1,2)fucosylation in PP M cells and F-ECs, respectively. (A) The proportions of NKM 16-2-4$^+$/UEA-1$^+$ cells in the proximal and distal villous epithelia of either day 1 PBS- or CT-administered (CT) WT C57BL/6J, Fut1-null and Fut2-null mice based on FCM as described in the Fig. 1 legend. Data are given as means ± SE (n = 3). Different letters indicate significant differences (P < 0.05) determined by Tukey's multiple comparison test. (B) The proportions of NKM 16-2-4$^+$ cells in the proximal PP domes based on histoplanimetrical analysis of CLSM images. WT, Fut1-null and Fut2-null mice were used after oral administration of either PBS or CT (day 1). Data are given as means ± SE (n = 3, 12–25 domes). Different letters indicate significant differences (P < 0.05) determined by Scheffé's multiple comparison test. (C) CLSM analysis for the whole-mount small intestinal epithelia of either naïve or day 1 CT-treated Fut1-null (naïve; 1, 2, CT; 3–8) and Fut2-null mice (naïve; 9, 10, CT; 11–16). Confocal images stained with NKM 16-2-4-FITC, UEA-1-TRITC and WGA-AF633 are shown by green, red and blue, respectively. Arrows and arrowheads indicate WGA$^-$ PP M cells and Fut1-dependent WGA$^+$ cells, respectively. Scale bars are 100 μm (1–4, 10–12), 50 μm (9), 20 μm (13–16) or 10 μm (5–8). (For interpretation of the references to colour in this figure legend, the reader is referred to the web version of this article.)

other hand, Fut2-null mice possessed few NKM 16-2-4$^+$/UEA-1$^+$ cells in the villous epithelia and the number of these cells was not increased upon oral CT administration (Fig. 4A and C; 10 and 12). PBS-administered Fut2-null mice showed 0.1% and 4.9% of NKM 16-2-4$^+$/UEA-1$^+$ cells in the proximal and distal villous epithelia, respectively, and CT-administered Fut2-null mice showed 0.3% and 5.3% in the proximal and distal villous epithelia, respectively (Fig. 4A).

In contrast to the villous epithelia, the PP FAE contained both types of fucosylated cells, dependent on either Fut1 or Fut2. In PBS-administered conditions, 2.0% and 6.3% of NKM 16-2-4$^+$ cells were observed in the proximal PP FAE of Fut1-null and Fut2-null mice, respectively (Fig. 4B). Oral CT administration did not notably induce α(1,2)fucosylation in the PP FAE of WT mice; CT-administered and PBS-administered WT mice contained 17.8% and 12.0% of NKM 16-2-4$^+$ cells, respectively, and there was no statistical difference between the two groups (Fig. 4B). However, both Fut1-null and Fut2-null mice showed significant induction of NKM 16-2-4$^+$ cells in the proximal PP FAE, with the proportion of positive cells being 60.5% and 21.0%, respectively (Fig. 4B). CLSM analysis further revealed that the fucosylation of M cells was dependent on Fut1, because WGA$^-$ M cells did not induce α(1,2)fucosylation and thus did not react with either NKM 16-2-4 or UEA-1 in Fut1-null mice (Fig. 4C; 1, 3 and 5–8: arrows) whereas they did react with these markers in Fut2-null mice (Fig. 4C; 9, 11 and 13–16: arrows) irrespective of oral CT administration. In addition, the fucosylation of F-ECs in the PP FAE was dependent on Fut2 because triple-positive cells (NKM 16-2-4$^+$/UEA-1$^+$/WGA$^+$ cells) were preferentially observed in the CT-administered Fut1-null mice (Fig. 4C; 3 and 5–8). Although a small number of Fut1-dependent WGA$^+$ cells were observed in the PP FAE of CT-administered Fut2-null mice (Fig. 4C; 13–16: arrowheads), they were distributed radially, accompanying abundant WGA$^-$ M cells on the PP dome (Fig. 4C; 11), and were distinguishable from the Fut2-dependent F-ECs that were distributed all over the dome (Fig. 4C; 3).

Taken together, these results indicate that α(1,2)fucosylation of PP M cells is dependent on Fut1 irrespective of IES, and that Fut2 is involved in α(1,2)fucosylation of F-ECs residing in both the PP FAE and villous epithelium in response to IES.

4. Discussion

In this study, we showed that intestinal environmental and biological stress induced F-ECs, which were recognized by NKM 16-2-4 and UEA-1, in both the PP FAE and the villous epithelium. However, such IES-induced F-ECs possessed a strong affinity for WGA (Fig. 2). In addition, F-ECs showed the same morphological characteristics as ECs such as columnar architecture, well-developed tall and dense microvilli (Supplementary Fig. S4), and did not possess *Salmonella* uptake-ability (Supplementary Fig. S5). Furthermore, F-ECs did not express glycoprotein 2 (Supplementary Fig. S6 and Table S1), recently identified as an M cell-specific molecule [17,25]. Therefore, F-ECs should be distinguished from typical M cells, and IES-induced α(1,2)fucosylation reflects only a phenotypic change of surface glycosylation pattern that is irrelevant to M-cell differentiation.

The requirements for different fucosylation-inducing enzymes clearly demonstrated a distinction between F-ECs and PP M cells: Fut1 is essential for the fucosylation associated with PP M cells while Fut2 is specifically involved in the fucosylation of IES-induced F-ECs in both the PP FAE and villous epithelium (Fig. 4). Although it has been reported that the expression of *Fut1* transcripts is rare and is not induced or altered in the small intestine by the transfer from germ-free to conventional conditions [11,18–20], these results are probably due to the low frequency of PP M cells throughout the small intestine. In contrast, it has been known that *Fut2* transcripts are induced in the small intestine, particularly in the ileum, of mice in response to colonization by commensal bacteria or treatment with a protein synthesis inhibitor [11,19]. Our present data, in which IES resulted in the induction of Fut2-dependent F-ECs, is consistent with and support these previous findings.

Fut1 and Fut2 provide insights into the involvement of IES in the development of not only F-ECs but also M cells. The PP dome epithelium consists of two cell lineages: one is derived from the dome-associated crypts and differentiates into either M cells or ECs, and the other is derived from villus-associated crypts and differentiates into ECs [26]. In addition, some studies have revealed a dynamic and plastic morphology of M cells; for example, the distinctive microfold and membranous structures occur transiently during the cell differentiation process, and M cell-lineage cells in their early and terminal development stages show the same morphological structure as ECs [27,28]. In this study, we showed a possibility that Fut1-dependent fucosylated cells are increased by IES (Fig. 4). These cells consisted of abundant PP M cells and a few WGA$^+$ EC-like cells, both of which were distributed radially on the dome. To this end, we suggest a possibility that Fut1-dependent cells are M cell-lineage cells derived from the dome-associated crypts that participate in the increase of M cells in response to IES, as described elsewhere [12–15]. In contrast to PP M cells, the fucosylation of villous M cells, like F-ECs, is regulated by Fut2 because α(1,2)fucosylation in the villi was not observed in Fut2-null but Fut1-null mice regardless of oral CT administration (Fig. 4 and Supplementary Table S1). However, IES alone would not influence the frequency of villous M cells because oral CT administration did not induce *Salmonella* uptake in the villi (Supplementary Fig. S5). It has recently been shown that receptor activator of nuclear factor-kappa B ligand (RANKL) is capable of the full development of both PP and villous M cells but RANKL-expressing inducer cells preferentially exist in the subepithelial dome of PPs [29]. Taken together, transient IES alone might be insufficient for the recruitment and/or induction of RANKL-expressing cells in the villi, and/or other factors might be required for the full development of villous M cells.

Although specific functions of F-ECs remain to be elucidated, our present study offers the possibility that Fut1-null and Fut2-null mice would provide a direct opportunity to examine *in vivo* the immuno-biological role of F-ECs and M cells, including their specific fucosylated glycans, towards a better understanding of the gut mucosal immune system.

Acknowledgments

We thank Dr. Osamu Igarashi for technical support and Dr. Rebecca Devon for editing the manuscript. This work was supported in part by Grants from the Ministry of Education, Science, Sports and Culture of Japan (H.K. and K.T.), and the Ministry of Health, Labour and Welfare of Japan (H.K.).

Appendix A. Supplementary data

Supplementary data associated with this article can be found, in the online version, at doi:10.1016/j.bbrc.2010.12.067.

References

[1] M.R. Neutra, A. Frey, J.P. Kraehenbuhl, Epithelial M cells: gateways for mucosal infection and immunization, Cell 86 (1996) 345–348.
[2] H. Hamada, T. Hiroi, Y. Nishiyama, et al., Identification of multiple isolated lymphoid follicles on the antimesenteric wall of the mouse small intestine, J. Immunol. 168 (2002) 57–64.
[3] R.L. Owen, A.L. Jones, Epithelial cell specialization within human Peyer's patches: an ultrastructural study of intestinal lymphoid follicles, Gastroenterology 66 (1974) 189–203.

[4] M.R. Neutra, N.J. Mantis, A. Frey, et al., The composition and function of M cell apical membranes: implications for microbial pathogenesis, Semin. Immunol. 11 (1999) 171–181.
[5] J.P. Kraehenbuhl, M.R. Neutra, Epithelial M cells: differentiation and function, Annu. Rev. Cell Dev. Biol. 16 (2000) 301–332.
[6] M.A. Clark, M.A. Jepson, N.L. Simmons, et al., Differential expression of lectin-binding sites defines mouse intestinal M-cells, J. Histochem. Cytochem. 41 (1993) 1679–1687.
[7] M.A. Clark, M.A. Jepson, N.L. Simmons, et al., Selective binding and transcytosis of Ulex europaeus 1 lectin by mouse Peyer's patch M-cells in vivo, Cell Tissue Res. 282 (1995) 455–461.
[8] M.H. Jang, M.N. Kweon, K. Iwatani, et al., Intestinal villous M cells: an antigen entry site in the mucosal epithelium, Proc. Natl. Acad. Sci. USA 101 (2004) 6110–6115.
[9] Y. Umesaki, M. Ohara, Factors regulating the expression of the neutral glycolipids in the mouse small intestinal mucosa, Biochim. Biophys. Acta 1001 (1989) 163–168.
[10] L. Bry, P.G. Falk, T. Midtvedt, et al., A model of host-microbial interactions in an open mammalian ecosystem, Science 273 (1996) 1380–1383.
[11] B. Lin, Y. Hayashi, M. Saito, et al., GDP-fucose: beta-galactoside alpha1,2-fucosyltransferase, MFUT-II, and not MFUT-I or -III is induced in a restricted region of the digestive tract of germ-free mice by host-microbe interactions and cycloheximide, Biochim. Biophys. Acta 1487 (2000) 275–285.
[12] M.W. Smith, P.S. James, D.R. Tivey, M cell numbers increase after transfer of SPF mice to a normal animal house environment, Am. J. Pathol. 128 (1987) 385–389.
[13] T.C. Savidge, M.W. Smith, P.S. James, et al., Salmonella-induced M-cell formation in germ-free mouse Peyer's patch tissue, Am. J. Pathol. 139 (1991) 177–184.
[14] C. Borghesi, M.J. Taussig, C. Nicoletti, Rapid appearance of M cells after microbial challenge is restricted at the periphery of the follicle-associated epithelium of Peyer's patch, Lab. Invest. 79 (1999) 1393–1401.
[15] T. Kucharzik, A. Lugering, N. Lugering, et al., Characterization of M cell development during indomethacin-induced ileitis in rats, Aliment. Pharmacol. Ther. 14 (2000) 247–256.
[16] J. Mach, T. Hshieh, D. Hsieh, et al., Development of intestinal M cells, Immunol. Rev. 206 (2005) 177–189.
[17] K. Terahara, M. Yoshida, O. Igarashi, et al., Comprehensive gene expression profiling of Peyer's patch M cells, villous M-like cells and intestinal epithelial cells, J. Immunol. 180 (2008) 7840–7846.
[18] S.E. Domino, N. Hiraiwa, J.B. Lowe, Molecular cloning, chromosomal assignment and tissue-specific expression of a murine alpha(1,2)-fucosyltransferase expressed in thymic and epididymal epithelial cells., Biochem. J. 327 (Pt 1) (1997) 105–115.
[19] M. Iwamori, S.E. Domino, Tissue-specific loss of fucosylated glycolipids in mice with targeted deletion of alpha(1, 2)fucosyltransferase genes, Biochem. J. 380 (2004) 75–81.
[20] B. Lin, M. Saito, Y. Sakakibara, et al., Characterization of three members of murine alpha1,2-fucosyltransferases: change in the expression of the Se gene in the intestine of mice after administration of microbes, Arch. Biochem. Biophys. 388 (2001) 207–215.
[21] S.E. Domino, L. Zhang, P.J. Gillespie, et al., Deficiency of reproductive tract alpha(1,2)fucosylated glycans and normal fertility in mice with targeted deletions of the FUT1 or FUT2 alpha(1,2)fucosyltransferase locus, Mol. Cell. Biol. 21 (2001) 8336–8345.
[22] T. Nochi, Y. Yuki, A. Matsumura, et al., A novel M cell-specific carbohydrate-targeted mucosal vaccine effectively induces antigen-specific immune responses, J. Exp. Med. 204 (2007) 2789–2796.
[23] I. Okayasu, S. Hatakeyama, M. Yamada, et al., A novel method in the induction of reliable experimental acute and chronic ulcerative colitis in mice, Gastroenterology 98 (1990) 694–702.
[24] T. Kunikata, H. Araki, M. Takeeda, et al., Prostaglandin E prevents indomethacin-induced gastric and intestinal damage through different EP receptor subtypes, J. Physiol. Paris 95 (2001) 157–163.
[25] K. Hase, K. Kawano, T. Nochi, et al., Uptake through glycoprotein 2 of FimH(+) bacteria by M cells initiates mucosal immune response, Nature 462 (2009) 226–230.
[26] A. Gebert, S. Fassbender, K. Werner, et al., The development of M cells in Peyer's patches is restricted to specialized dome-associated crypts, Am. J. Pathol. 154 (1999) 1573–1582.
[27] S. Onishi, T. Yokoyama, K. Chin, et al., Ultrastructural study on the differentiation and the fate of M cells in follicle-associated epithelium of rat Peyer's patch, J. Vet. Med. Sci. 69 (2007) 501–508.
[28] F. Sierro, E. Pringault, P.S. Assman, et al., Transient expression of M-cell phenotype by enterocyte-like cells of the follicle-associated epithelium of mouse Peyer's patches, Gastroenterology 119 (2000) 734–743.
[29] K.A. Knoop, N. Kumar, B.R. Butler, et al., RANKL is necessary and sufficient to initiate development of antigen-sampling M cells in the intestinal epithelium, J. Immunol. 183 (2009) 5738–5747.

Rev. Med. Virol. 2010; **20**: 77–92.
Published online 4 January 2010 in Wiley InterScience
(www.interscience.wiley.com)
DOI: 10.1002/rmv.637

Reviews in Medical Virology

REVIEW

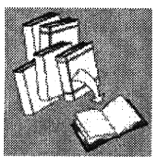

Anti-retroviral activity of TRIM5α

Emi E. Nakayama* and Tatsuo Shioda

Department of Viral Infections, Research Institute for Microbial Disease, Osaka University, 3-1 Yamadaoka, Suita, Osaka 565-0871, Japan

SUMMARY

Human immunodeficiency virus type 1 (HIV-1) shows a very narrow host range limited to humans and chimpanzees. Experimentally, HIV-1 does not infect Old World monkeys, such as rhesus (Rh) and cynomolgus (CM) monkeys, and fails to replicate in activated CD4 positive T lymphocytes obtained from these monkeys. In contrast, simian immunodeficiency virus isolated from a macaque monkey (SIVmac) can replicate well in both Rh and CM. In 2004, tripartite motif 5α (TRIM5α) was identified as a host factor which plays an important role in the restricted host range of HIV-1. Rh and CM TRIM5α restrict HIV-1 infection but not SIVmac, while in comparison, anti-viral activity of human TRIM5α against those viruses is very weak. TRIM5α consists of the RING, B-box 2, coiled-coil and SPRY (B30.2) domains. The RING domain is frequently found in E3 ubiquitin ligase and TRIM5α is degraded via the ubiquitin-proteasome pathway during HIV-1 restriction. TRIM5α recognises the multimerised capsid (viral core) of an incoming virus by its α-isoform specific SPRY domain and is believed to be involved in innate immunity to control retroviral infection. Differences in amino acid sequences in the SPRY domain of TRIM5α of different monkey species were found to affect species-specific restriction of retrovirus infection, while differences in amino acid sequences in the viral capsid protein determine viral sensitivity to restriction. Accurate structural analysis of the binding surface between the viral capsid protein and TRIM5α SPRY is thus required for the development of new antiretroviral drugs that enhance anti-HIV-1 activity of human TRIM5α. Copyright © 2010 John Wiley & Sons, Ltd.

Received: 24 August 2009; Revised: 10 September 2009; Accepted: 10 September 2009

INTRODUCTION

Human immunodeficiency virus type 1 (HIV-1), a major causative agent of acquired immunodeficiency syndrome (AIDS), belongs to the genera lentivirus of the family *Retroviridae*. HIV-1 is thought to have been introduced into the human population from chimpanzees [1] and has a very narrow host range limited to humans and chimpanzees. Experimentally, HIV-1 fails to replicate in activated CD4 positive T lymphocytes obtained from Old World monkey (OWM)s, such as rhesus (Rh) [2,3] and cynomolgus (CM) monkeys [4,5]. In contrast, another lentivirus simian immunodeficiency virus isolated from sooty mangabey (SIVsm) and simian immunodeficiency virus isolated from African green monkey (SIVagm) replicate in their natural hosts [6]. Simian immunodeficiency virus isolated from a macaque monkey (SIVmac), with a genome that has 55% nucleotide sequence homology to that of HIV-1, was evolved from SIVsm in macaques in captivity, and replicates efficiently in Rh [2,3] and CM [4,5]. The restricted host range of HIV-1 has greatly hampered its use in animal experiments, and, thus the development of prophylactic vaccines against HIV-1 infection. In 2004, tripartite motif 5α (TRIM5α) was identified as a host factor that plays an important role in the restricted host range of HIV-1. In this review

*Corresponding author: E. E. Nakayama, Department of Viral Infections, Research Institute for Microbial Disease, Osaka University, 3-1 Yamadaoka, Suita, Osaka 565-0871 Japan.
E-mail: emien@biken.osaka-u.ac.jp

Abbreviations used

A, alanine; AGM, African green monkey; AIDS; acquired immune deficiency syndrome; APOBEC, ApoB mRNA editing catalytic sub unit; CA, capsid protein; CM, cynomolgus monkey; CsA, cyclosporine A; CypA, cyclophilin A; HIV-1, human immunodeficiency virus type 1; HIV-2, human immunodeficiency virus type 2; L4/5, a loop between α-helices 4 and 5 of CA; L6/7, a loop between α-helices 6 and 7 of CA; NC, nucleocapsid protein; N-MLV, N-tropic murine leukemia viruses; OWM, Old World monkey; P; proline; Q, glutamine; R, arginine. Rh, rhesus monkey; RING, really interesting new gene; SPRY, a sequence repeat in the dual-specificity kinase splA and ryanodine receptors; SHIV, Chimeric virus between SIVmac and HIV-1; SIVmac, simian immunodeficiency virus isolated from macaque; TRIM5α, tripartite motif 5α; TRIMCyp, TRIM5 and CypA fusion protein; VL, viral load; VSV-G, vesicular stomatitis virus glycoprotein

article, recent findings in TRIM5α research are summarised and details of the molecular mechanisms of HIV-1 restriction by TRIM5α are discussed.

IDENTIFICATION OF TRIMα AS A RESTRICTION FACTOR AGAINST HIV-1 IN OWM CELLS

Several earlier studies have suggested that the block of HIV-1 replication in OWM cells occurs at a post-entry step [2,3,7] and appears to result from a failure to initiate reverse transcription [3]. Studies of HIV-1 and SIVmac chimera have suggested that restriction determinants lie within the HIV-1 p24 capsid protein (CA) [8–11]. The block was still observed in CD4-negative monkey cells infected with HIV-1 pseudotyped with vesicular stomatitis virus glycoprotein (VSV-G) (Figure 1) but was overridden by high-dose infection with VSV-G-pseudotyped virus or virus-like particles lacking genomic RNA [12–15]. Importantly, resistance against HIV-1 infection was shown to be dominant in heterokaryons between human and OWM cells, suggesting the presence of inhibitory factor(s) against HIV-1 infection in OWM cells [14].

In 2004, the screening of a Rh cDNA library identified TRIM5α, a component of cytoplasmic bodies, as a factor that confers resistance to HIV-1 infection [16]. Rh and CM TRIM5α restrict HIV-1 infection but not SIVmac [16,17]. In contrast, human TRIM5α is almost powerless to restrict the aforementioned viruses, but potently restricts N-tropic murine leukemia viruses (N-MLV), which belong to genera Gammaretrovirus. It was previously shown that human cells are resistant to infection with N-MLV and the presence in human

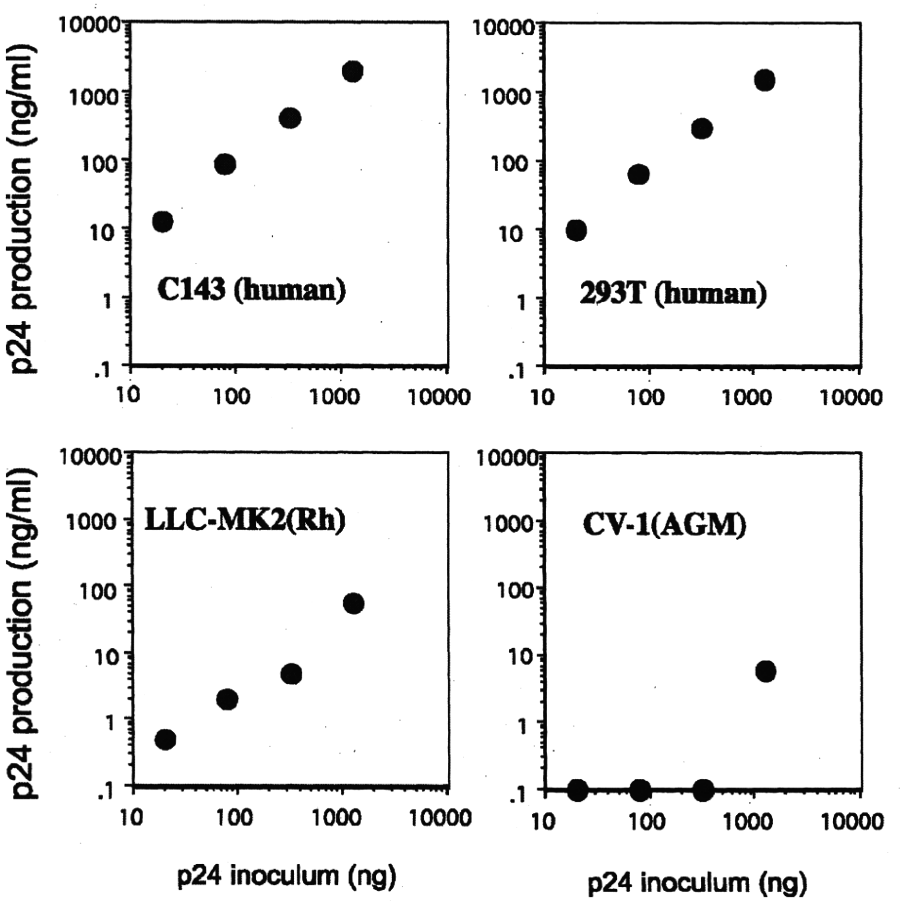

Figure 1. Old World monkey (OWM) cells are resistant to HIV-1 infection. Human C143 and 293T cell line were highly sensitive to vesicular stomatitis virus glycoprotein-pseudotyped HIV-1 infection, while rhesus monkey (Rh) LLC-MK2 and African green monkey (AGM) CV1 cell lines were resistant. When extremely high doses of virus were inoculated, cells became sensitive to infection, suggesting that the intrinsic restriction factor(s) were saturated with virions

cells of a virtual restriction factor known as Ref1 was posited. It is now widely accepted that the presence of human TRIM5α substantiates that of the restriction factor Ref1 [18–21]. On the other hand, African green monkey (AGM) cells have been shown to possess another factor, Lv1, which restricts both HIV-1 and SIVmac infection and we and others identified the factor as AGM TRIM5α [17,18]. AGM TRIM5α fails to restrict SIVagm. Unlike humans and other OWMs, pig-tailed monkeys lack expression of TRIM5α, but instead express TRIM5θ and TRIM5η, which lack anti-HIV-1 activity [22]. It is now known that type I interferons up-regulate the transcription of TRIM5α in human [23] and monkey cells [24] and this in turn enhances restriction activity against N-MLV [24,25].

TRIPARTITE MOTIF OF TRIM5α

The human genome contains approximately 70 genes of the TRIM family, which characteristically encode a tripartite protein motif [26–29]. This tripartite motif consists of a really interesting new gene (RING) zinc-finger domain, one or two B-box zinc-finger domains and an α-helical coiled-coil domain. *TRIM* genes are scattered throughout the human genome, while the *TRIM5* locus lies in a small cluster of four related *TRIM* genes including *TRIM6*, *TRIM34* and *TRIM22* [30]. Although the functions of most TRIM family members are still unknown, several TRIM proteins including TRIM1, TRIM19 (PML), TRIM22 and TRIM32 reportedly have anti-viral effects (reviewed in Reference [26]). Especially, TRIM19 can suppress broad spectrum of viruses such as herpes simplex virus type 1 and lymphocytic choriomeningitis virus [26]. TRIM21 is a trimeric protein that binds IgG Fc via the C-terminal of the B30.2 domain [31]. Subcellular localisation of the TRIM proteins varies among members of the TRIM family [27]: TRIM19, 24 and 27 are associated with nuclear bodies and TRIM1 and 18 with microtubules. TRIM5α was first identified as a cytoplasmic body protein [27], but diffuse expression in cytoplasm has proved important for its anti-viral activity [32].

As shown in Figure 2, TRIM5α consists of RING, B-box 2, coiled-coil and SPRY (B30.2) domains [27]. The RING domain containing proteins possess E3 ubiquitin ligase activity [33] and the intact RING domain of TRIM5α was thought to be essential for retrovirus restriction (see below). The intact

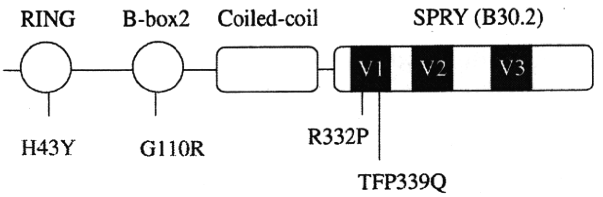

Figure 2. TRIM5α protein. TRIM5α protein contains RING, B-box 2, and coiled-coil domains, the three signature domains of the TRIM gene family. The α isoform possesses a SPRY domain sometimes referred to as a B30.2 domain. V1, V2 and V3 denote variable regions 1, 2 and 3 among monkey species, respectively. A histidine-to-tyrosine substitution at position 43 (H43Y) and a glycine-to-arginine substitution at position 110 (G110R) of human TRIM5 (shown in red) modulate anti-viral activity against retroviruses *in vitro*. Position 332 in human TRIM5α is arginine (R) and no polymorphism was reported in human genome. In contrast, proline (P)-to-glutamine (Q) substitution in rhesus monkey (Rh) and R-to-P or -Q substition in sooty mangabeys were found (R332P/Q). A 339th-TFP-341st to -Q polymorphism (TFP339Q) that reduces the anti-human immunodeficiency virus type 2 (HIV-2) activity was found in Rh TRIM5α

B-box 2 domain is also required for TRIM5α mediated antiviral activity since the restrictive activity of TRIM5α is diminished by several amino acid substitutions in the B-box 2 domain [34]. TRIM5α has been shown to form a trimer [35,36] or a dimer [37,38], while the B-box 2 domain mediates higher-order self-association of Rh TRIM5α oligomers. This self-association increases the efficiency of TRIM5α binding to the retroviral CA, thus potentiating restriction of retroviral infection [39,40]. The coiled-coil domain of TRIM5α has been identified as important for the formation of homo-oligomers [35], and homo-oligomerisation of TRIM5α as essential for antiviral activity [36,41]. The SPRY domain is specific for an α isoform among at least three splicing variants transcribed from the *TRIM5* gene. *TRIM5γ* and TRIM5δ lack the SPRY domain because of alternative splicing and their functions remain unknown. Exogenously expressed TRIM5γ is unstable [42] and over-expression of the TRIM5 protein lacking the SPRY domain dominant-negatively suppresses the anti-viral activity of the intact TRIM5α through hetero-oligomerisation [41,42].

SPRY (B30.2) DOMAIN OF TRIM5α

The C-terminal halves of TRIM family proteins are variable and half of them, including the TRIM5α, encode B30.2 (SPRY or PRYSPRY) domain [27]. Soon after identification of TRIM5α as a restriction

factor of Rh, many studies found that differences in the amino acid sequences in the TRIM5α SPRY domain of different monkey species affect the species-specific restriction of retrovirus infection [17,43–50].

Studies on human and Rh recombinant TRIM5αs have shown that the determinant of the species-specific restriction against HIV-1 infection resides in variable region 1 (V1) of the SPRY domain [43,44]. We found that 17-amino-acid residues and adjacent 20-amino-acid duplication in the V1 of AGM TRIM5α determined species-specific restriction against SIVmac [17]. Interestingly, a study comparing human and Rh TRIM5α showed that a single change from arginine (R) to proline (P) at the 332nd position in the V1 of human TRIM5α (R332P) conferred potent restriction ability against not only HIV-1 but also SIVmac239 [49,50]. In the case of human immunodeficiency virus type 2 (HIV-2) infection, we found that three amino acid residues of TFP at the 339th to 341st positions of Rh TRIM5α V1 are important for restricting particular HIV-2 strains which are still resistant to CM TRIM5α [45].

A study comparing orangutan and gorilla TRIM5αs showed that two amino acid residues at the 385th and 389th positions in the variable region 2 (V2) of SPRY domain of orangutan TRIM5α are important for restriction against HIV-1 and SIVmac [46]. We found that one amino acid residue at the 385th (baboon) or 383rd (CM) position in V2 of the SPRY domain of TRIM5α also affects its restriction ability against HIV-2 [47]. A computer-assisted 3-D model of the TRIM5α SPRY domain showed that V1 and V2 are located in the loops at the surface of the SPRY domain and the structure composed of the V1 and V2 regions is thought to be important for TRIM5α restriction (Figure 3).

Furthermore, a comparison of human and Rh TRIM5α restriction of N-MLV showed that the amino acid residues of human TRIM5α at the 409th and 410th positions in the variable region 3 (V3) of SPRY domain are important for restricting N-MLV [48].

Finally, biochemical studies have shown that TRIM5α associates with CA in detergent-stripped N-MLV virions [51] or with an artificially constituted HIV-1 core structure composed of the capsid-nucleocapsid (CA-NC) fusion protein in a SPRY domain dependent manner [52]. The SPRY domain is thus thought to recognise viral cores.

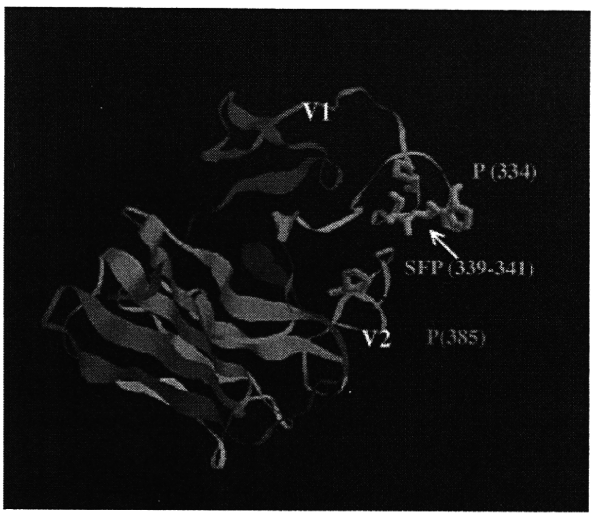

Figure 3. Structure of SPRY domain of TRIM5α. This 3-D model of the baboon SPRY domain was constructed with a homology-modeling technique based on mouse TRIM21 [131]. Position 332 in human TRIM5α is the same as position 334 in baboon TRIM5α. SFP motif in V1 and P residue at position 385 in V2 are shown

VIRAL DETERMINANT OF TRIM5α SENSITIVITY

To determine the CA region that interacts with TRIM5α, we focused on HIV-2, which strongly resembles SIVmac [53]. Previous studies have shown that HIV-2 strains vary widely in their ability to grow in OWM cells such as baboon, Rh and CM [54–58] and HIV-2 isolates with various growth capabilities in OWM cells were evaluated for their sensitivity to CM TRIM5α [59]. We found that viral sensitivity to CM TRIM5α inversely correlates with growth capability in OWM cells. Sequence analysis showed that the CM TRIM5α-sensitive viruses had proline (P) at the 119th or 120th position of CA, while the CM TRIM5α-resistant viruses had either alanine (A) or glutamine (Q) at the same position. Replacing the proline of a CM TRIM5α-sensitive HIV-2 molecular clone with either alanine or glutamine changed the phenotype from sensitive to resistant (Figure 4) and the mutant viruses replicated well in the presence of CM TRIM5α. The reverse was observed when the glutamine of a resistant SIVmac molecular clone was replaced with proline. Similar results, although to a lesser extent, were observed when human TRIM5α was used [59]. These results indicate that a single amino acid at the 119th or 120th

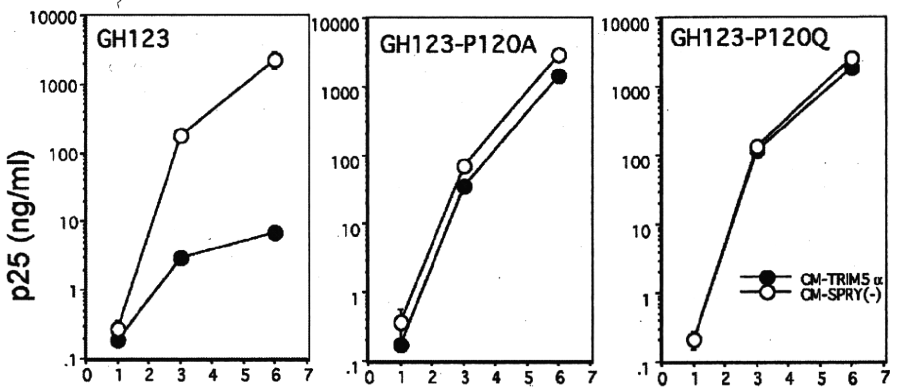

Figure 4. A single amino acid of HIV-2 capsid (CA) affects its replication in the presence of cynomolgus monkey (CM) TRIM5α. HIV-2 GH123 replication was restricted in CM-TRIM5α expressing human CD4 T cell line (CM-TRIM5α; black circles). The mutant GH123-P120A and GH123-P120Q viruses were generated by changing a single amino acid proline (P) at position 120 of GH123 CA to alanine (A) or glutamine (Q). These mutant viruses replicated in CM-TRIM5α expressing cells as efficiently as in cells lacking TRIM5α expression (CM-SPRY(-); white circles)

position of HIV-2 CA drastically affects viral sensitivity to TRIM5α.

A computer-assisted 3-D model of the HIV-2 CA showed that the 119th or 120th position is located in the loop between α-helices 6 and 7 (L6/7, Figure 5A). Previously, a single amino acid substitution at the 110th position of N-MLV CA had been shown to determine viral susceptibility to Fv1 [60], another restriction factor present in certain strains of mice [61] as well as to Ref1 (human TRIM5α) [18,20,21]. The recently published 3-D structure of MLV CA [62,63] revealed that the 110th position of N-MLV CA is located at a position in the surface-exposed loop analogous to the 119th or 120th position of HIV-2 CA. As mentioned above, V3 in the SPRY domain of human TRIM5α reportedly plays an important role in the restriction of N-MLV [48], whereas V1 in the SPRY domain of OWM TRIM5αs determines restriction specificity against HIV-1 and SIVmac [17,43,44,49,50]. These results indicate that the surface-exposed loop of CA is important for recognition by cellular restriction factors, even though critical amino acid residues in human TRIM5α for N-MLV restriction are different from those in CM TRIM5α for HIV-2.

HIV-2 is assumed to have originated from SIVsm as the result of zoonotic events involving monkeys and humans [53]. Almost all the SIV isolates in the Los Alamos database contain glutamine at the position corresponding to the 119th or 120th position of HIV-2 CA. In contrast, HIV-2 strains possess a mixture of glutamine, alanine and proline at the corresponding position. It is thus likely that glutamine-to-alanine or glutamine-to-proline substitutions occurred after the hypothesised zoonotic transfer of virus from monkeys to humans. According to this hypothesis, a single nucleotide change in the second position of the glutamine codons (CAA or CAG) would generate proline codons (CCN), and an additional single nucleotide change in the first position in CCN would generate alanine codons (GCN). Most likely, the glutamine residue first changed into proline residue in humans as a result of certain pressures from the human immune system in the absence of strong pressure from OWM TRIM5α. Since HIV-2 strains with proline residue show moderate sensitivity to human TRIM5α, an additional change would have to have occurred to generate alanine residue for better replication in human populations.

Does amino acid residue at the 119th or 120th position in HIV-2 CA affect HIV disease in infected individuals? It is known that HIV-1 and HIV-2 have distinct natural histories, levels of viremia, transmission rates and disease associations despite strong sequence homology between the two viruses [64]. Although some HIV-2-infected patients progress to AIDS, the infection is controlled in the majority of patients [65,66] and those with low viral load (VL) have a much longer survival [67]. A detailed sequence analysis of HIV-2 CA variations within a large community cohort